The Canadian Mineralogist
Vol. 34, pp. 845-880 (1996)

U^{6+} MINERALS AND INORGANIC PHASES: A COMPARISON AND HIERARCHY OF CRYSTAL STRUCTURES

PETER C. BURNS[1], MARK L. MILLER AND RODNEY C. EWING

Department of Earth and Planetary Sciences, The University of New Mexico, Albuquerque, New Mexico 87131-1116, U.S.A.

ABSTRACT

A hierarchical structural classification is developed for U^{6+} minerals and inorganic phases, based on the polymerization of coordination polyhedra of higher bond-valence. The U^{6+} cation is usually present as part of the approximately linear $(U^{6+}O_2)^{2+}$ uranyl (*Ur*) ion, which is coordinated by four, five or six anions (ϕ: O^{2-},OH^-,H_2O), with the oxygen atoms of the uranyl ion forming the apices of square, pentagonal and hexagonal bipyramids, respectively. The uranyl ion <U–O> bond-lengths are ~1.8 Å in each coordination polyhedron, and the equatorial <U–O> bond-lengths for $Ur\phi_4$, $Ur\phi_5$ and $Ur\phi_6$ polyhedra are 2.26(8), 2.34(10) and 2.46(12) Å, respectively. Inorganic oxide phases in which U^{6+} plays a significant structural role are considered. A total of one hundred and eighty structures (of which fifty-six are of minerals) have been placed in the hierarchy of structures: one hundred and six (forty-three minerals) contain infinite sheets of polyhedra, nineteen (five minerals) contain eight different infinite chains of polyhedra, twenty-two (five minerals) contain ten different finite clusters of polyhedra, seven (no minerals) contain isolated polyhedra, and twenty-six (three minerals) structures contain frameworks of polyhedra. The sheets of polyhedra that occur in one hundred and six structures are classified according to the details of their topological arrangements of anions within the sheets, with twenty-nine different sheet anion-topologies observed, but six of these topologies account for 82% of observed sheets.

Keywords: uranyl, uranium, actinide, structure hierarchy, structure classification, crystal structures, nuclear waste.

SOMMAIRE

Nous proposons une classification structurale hiérarchique des minéraux et des phases inorganiques contenant U^{6+}, fondée sur la polymérisation des polyèdres de coordinence ayant la valence de liaison la plus élevée. Le cation U^{6+} est normalement présent sous forme de l'ion uranyle (*Ur*), $(U^{6+}O_2)^{2+}$, agencement approximativement linéaire, qui est entouré de quatre, cinq ou six anions (ϕ: O^{2-},OH^-,H_2O), les atomes d'oxygène de l'ion uranyle formant les sommets de bipyramides carrées, pentagonales et hexagonales, respectivement. Les longueurs de la liaison <U–O> de l'ion uranyle sont d'environ 1.8 Å dans chacun de ces polyèdres, et celle des liaisons <U–O> équatoriales $Ur\phi_4$, $Ur\phi_5$ et $Ur\phi_6$ sont 2.26(8), 2.34(10) et 2.46(12) Å, respectivement. Nous considérons aussi les oxydes inorganiques dans lesquels le U^{6+} joue un rôle structural important. En tout, cent quatre-vingt structures, dont cinquante-six sont celles de minéraux, sont placées dans une hiérarchie. De ce nombre, cent-six (quarante-trois minéraux) contiennent des feuillets infinis de polyèdres, dix-neuf (cinq minéraux) contiennent huit chaînes infinies de polyèdres distinctes, vingt-deux (cinq minéraux) contiennent dix groupements finis distincts de polyèdres, sept (sans exemple dans la nature) contiennent des polyèdres isolés, et vingt-six (trois minéraux) contiennent des trames tri-dimensionnelles de polyèdres. Nous classifions les feuillets de polyèdres retrouvés dans les cent-six structures selon les détails de leurs agencements topologiques d'anions à l'intérieur d'un feuillet. Il en résulte vingt-neuf topologies distinctes des anions, mais six de celles-ci rendent compte de 82% de tous les agencements en feuillets observés.

(Traduit par la Rédaction)

Mots-clés: uranyle, uranium, actinide, hiérarchie structurale, classification structurale, structure cristalline, déchets nucléaires.

INTRODUCTION

Most uranium-bearing minerals contain U^{6+}, the oxidized form of uranium. The U^{6+} cation is almost always present as part of an approximately linear $(U^{6+}O_2)^{2+}$ uranyl ion (Evans 1963). Where found in crystal structures, the uranyl ion is coordinated by four, five or six anions, in an approximately coplanar arrangement (Fig. 1). Although the U cation has a formal valence of +6, the valence of the uranyl ion is only approximately +2; thus $Ur\phi_4$, $Ur\phi_5$, and $Ur\phi_6$ polyhedra (*Ur*: uranyl ion, ϕ: O^{2-}, OH^-, H_2O) may polymerize with other $Ur\phi_n$ polyhedra or polymerize with other cation coordination polyhedra to form complex structures without violating the valence-sum rule (Brown 1981). There are 170 recognized mineral species listed in Fleischer & Mandarino (1991) that contain U^{6+} as a necessary structural constituent. Of

[1]*Present address:* Department of Geology, University of Illinois at Urbana-Champaign, 245 Natural History Building, 1301 West Green Street, Urbana, Illinois 61801, U.S.A.

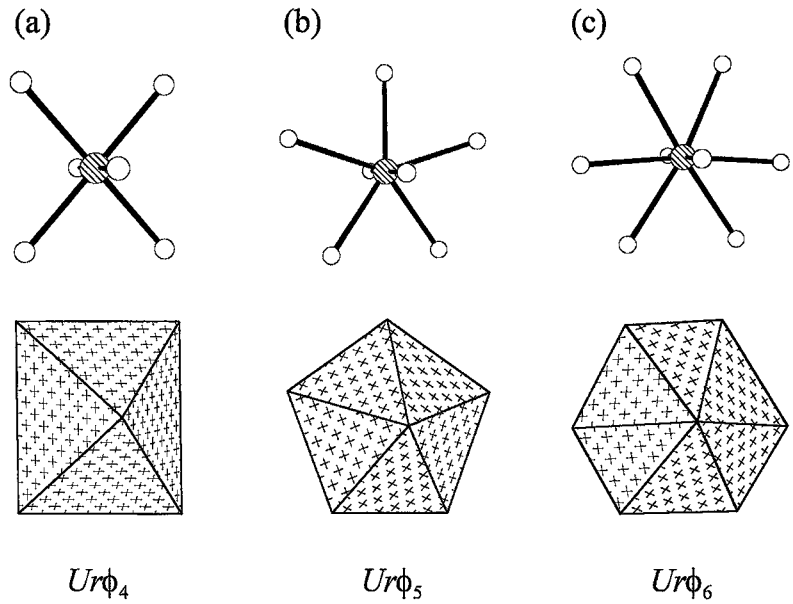

FIG. 1. The three types of $Ur\phi_n$ polyhedra (*Ur*: uranyl ion, ϕ: O^{2-},OH^-,H_2O). U^{6+} cations are shown as circles shaded with parallel lines, and anions are shown as open circles.

these, the structures are known and refined for 56. In addition, the structures of about 124 non-mineral U^{6+} phases are known. Here, we propose a hierarchy of structures for U^{6+} inorganic phases, including minerals.

The organization of crystal structures into hierarchies is not a new concept; Bragg (1930) first classified silicate structures based upon the polymerization of $(Si,Al)O_4$ tetrahedra, and this scheme was later generalized to include structures on the basis of the polymerization of any tetrahedra by Zoltai (1960) and Liebau (1985). The organization of U^{6+} structures into a hierarchy serves to order our current knowledge, and it also facilitates comparisons of the structures. This organization should be a significant aid during the determination of unknown crystal structures. Structural schemes also provide considerable insight into the underlying controls of bond topology (Hawthorne 1983, 1990) and mineral paragenesis (Moore 1965, 1973, Hawthorne 1985).

Recently, U^{6+} minerals and phases have received increased attention because they form as alteration products on uraninite under oxidizing conditions (Finch & Ewing 1992) and on the UO_2 of spent nuclear fuel in experimental studies of corrosion (Wronkiewicz *et al.* 1992). Under oxidizing conditions, such as those found in the proposed nuclear-waste repository at Yucca Mountain, Nevada, UO_2 is unstable, and the rate of alteration in the presence of water is likely to be appreciable (Murphy & Pabalan 1995). Thus, the oxidized products of alteration, mainly U^{6+} phases, will govern the release rate of radionuclides. A systematic, structural understanding of this rather large and complex group of minerals and phases is required in order to: (*i*) simply identify phases, particularly under the difficult conditions required in experiments with highly active spent nuclear fuel; (*ii*) evaluate the ability of different structures to act as effective host-phases for fission products (*e.g.*, Sr and Cs) and transuranic elements (*e.g.*, Np, Pu, Am, Cm); (*iii*) determine the expected paragenesis based on structural relationships and to evaluate the thermodynamic stability of these phases. The large majority of these phases may be classified as sheet structures; thus, it may be possible to calculate thermodynamic parameters (*e.g.*, solubility products) based on ideal structure-types and sheet-stacking arrangements.

GEOMETRIES OF URANYL POLYHEDRA

In crystal structures, the $(UO_2)^{2+}$ uranyl ion is coordinated by four, five or six anions, such that the coordinating anions are approximately coplanar with the U^{6+} cation, and the oxygen atoms that are part of the uranyl ion are the apices of square, pentagonal and hexagonal bipyramids (Fig. 1). As first noted by Evans (1963), the $Ur\phi_5$ polyhedron is the most common mode of accommodation of U^{6+} in solids.

The <U–O> bond-lengths in the uranyl ions are ~1.8 Å and are essentially insensitive to the coor-

dination of the uranyl ion. The O–U–O bond-angle of the uranyl ion is generally close to being linear, with divergence from linearity seldom exceeding 4°. The equatorial <U^{6+}–O> bond-lengths are dependent on coordination number; averages derived from 134 well-refined structures are $Ur\phi_4$ = 2.26(8) (44 polyhedra), $Ur\phi_5$ = 2.34(10) (125 polyhedra) and $Ur\phi_6$ = 2.46(12) Å (39 polyhedra). Assuming ideal bond-angles, and coplanarity of equatorial anions, one may calculate ideal equatorial edge-lengths: 3.20, 2.75 and 2.46 Å for $Ur\phi_4$, $Ur\phi_5$ and $Ur\phi_6$ polyhedra, respectively.

General Considerations

Smith (1984) presented a crystal-chemical classification of U^{6+} and U^{4+} minerals. Minerals were grouped on the basis of identities of the principal cations in the structure, and additional divisions within each chemical class were based upon structural criteria. The work of Smith (1984) represents an important step forward in the understanding of U minerals, in part because it places each mineral in a geological context.

Hawthorne (1983, 1985) has proposed that mineral structures can be ordered according to the polymerization of those cation polyhedra of higher bond-valence. Hawthorne (1985, 1990) used this idea to set up a hierarchy of structures for minerals based upon tetrahedrally and octahedrally coordinated cations. Here we adopt a similar approach for U^{6+} inorganic structures. The structural hierarchy that we propose is generally based upon the polymerization of those cation polyhedra of higher bond-valence, including, most importantly, U^{6+} polyhedra, but also including all other cation polyhedra of higher bond-valence. Usually the placement of a structure in the hierarchy is independent of the presence of hydrogen bonds or polyhedra containing mono- or divalent cations. However, it is our intent to illustrate similarities among structures, so it is in some cases appropriate to include polyhedra of low-valence cations when placing structures into the hierarchy. This is the case when a low-valence cation occupies a polyhedron that is similar to a U^{6+} polyhedron, resulting in a structural unit that is graphically identical to the structural unit (which does not contain a low-valence cation) in another structure.

As the anions that coordinate the uranyl ion are invariably close to being coplanar, and the bond-valence requirements of the oxygen atoms that are part of the uranyl ion are approximately satisfied without further bonding, geometrical constraints and the bonding of coordinating anions to two or three uranyl ions commonly result in polymerization to form infinite sheets. Of the structures considered here, ~60% are based upon infinite sheets. Chemical constraints, such as the relative amounts of uranium *versus* other cations in the structure, and the inclusion of monovalent anions (*i.e.*, Cl^-, F^-) or H_2O groups may reduce the degree of polymerization, resulting in structures that are based on infinite chains of polyhedra, finite clusters of polyhedra, or isolated polyhedra, in the extreme case. In addition, polymerization in the third dimension occurs, resulting in framework structures.

In most cases, the assignment of a structure to one of the principal structural classes (*i.e.*, infinite sheet, infinite chain, finite cluster, isolated polyhedron, framework) is straightforward. In structures containing sheets, the sheets of polyhedra are usually linked through low-valence cations or hydrogen bonds. However, in several structures, sheets of polyhedra link together by sharing anions, producing a framework. In these structures, the bonding is generally substantially stronger within the sheets than between the sheets, and the uranyl ion is usually oriented perpendicular to the sheet direction. In addition, such structures invariably contain sheets that are similar (or identical) to the sheets that occur isolated in other structures. Thus, we classify such structures as sheet structures rather than frameworks; the term *framework* is reserved for structures that have similar bond-strengths in all three dimensions.

In this work, only the structures of inorganic oxide phases are considered; structures of metal–organic phases are excluded. Only phases in which U^{6+} plays a significant structural role are considered, and only those for which crystal-structure data are available are included. Phases that are assumed to be isostructural with a phase for which the structure is known, but for which there are no structure data, are excluded.

In many cases, the chemical formulae used in the text and tables have been modified from those of the original authors so as to emphasize structural features and to facilitate comparison. All structures classified are listed in Tables 1 to 9, and only billietite is listed twice, as the structure of billietite contains two distinct sheets of polyhedra. In Tables 7 and 8, double lines are used to separate structures that contain different clusters and chains, respectively. In Tables 1 to 6, double lines separate structures that have sheets with different anion-topologies, and dotted lines separate structures with distinct sheets, but the same anion-topology.

Throughout this paper, *Ur* refers to the $(UO_2)^{2+}$ uranyl ion, and ϕ is O^{2-}, OH^- or H_2O. Thus, $Ur\phi_4$, $Ur\phi_5$ and $Ur\phi_6$ designate U^{6+} (as part of the uranyl ion) in square bipyramidal, pentagonal bipyramidal and hexagonal bipyramidal coordinations, respectively. The oxygen atoms that are part of the uranyl ion are designated O_{Ur}.

Infinite Sheets and Anion-Topologies

Crystal structures that contain uranyl polyhedra most often are based upon infinite sheets of edge- and corner-sharing polyhedra. These sheets may contain

only U^{6+} polyhedra, and in some of these cases the sheet contains more than one type of U^{6+} polyhedron. However, many structures are based upon complex heteropolyhedral sheets that contain, in addition to U^{6+} polyhedra, other cation polyhedra. One hundred and six U^{6+} phases are known to adopt a structure that is based on infinite sheets of polyhedra, thus the classification and comparison of these sheets are a challenge.

One particularly instructive way to compare and group these sheets is to consider the topological arrangement of the anions that occur *within* the sheets (Miller *et al.* 1995, 1996). The procedure used to identify the sheet's *anion-topology* is best illustrated by an example. Consider the sheet shown in Figure 2a. The anion-topology may be obtained as follows: (1) Each anion that is not bonded to at least two cations within the sheet, and is not an equatorial anion of a bipyramid or pyramid within the sheet, is removed from further consideration (Fig. 2c). (2) Cations are removed, along with all cation–anion bonds, leaving an array of unconnected anions (Fig. 2d). (3) Anions are

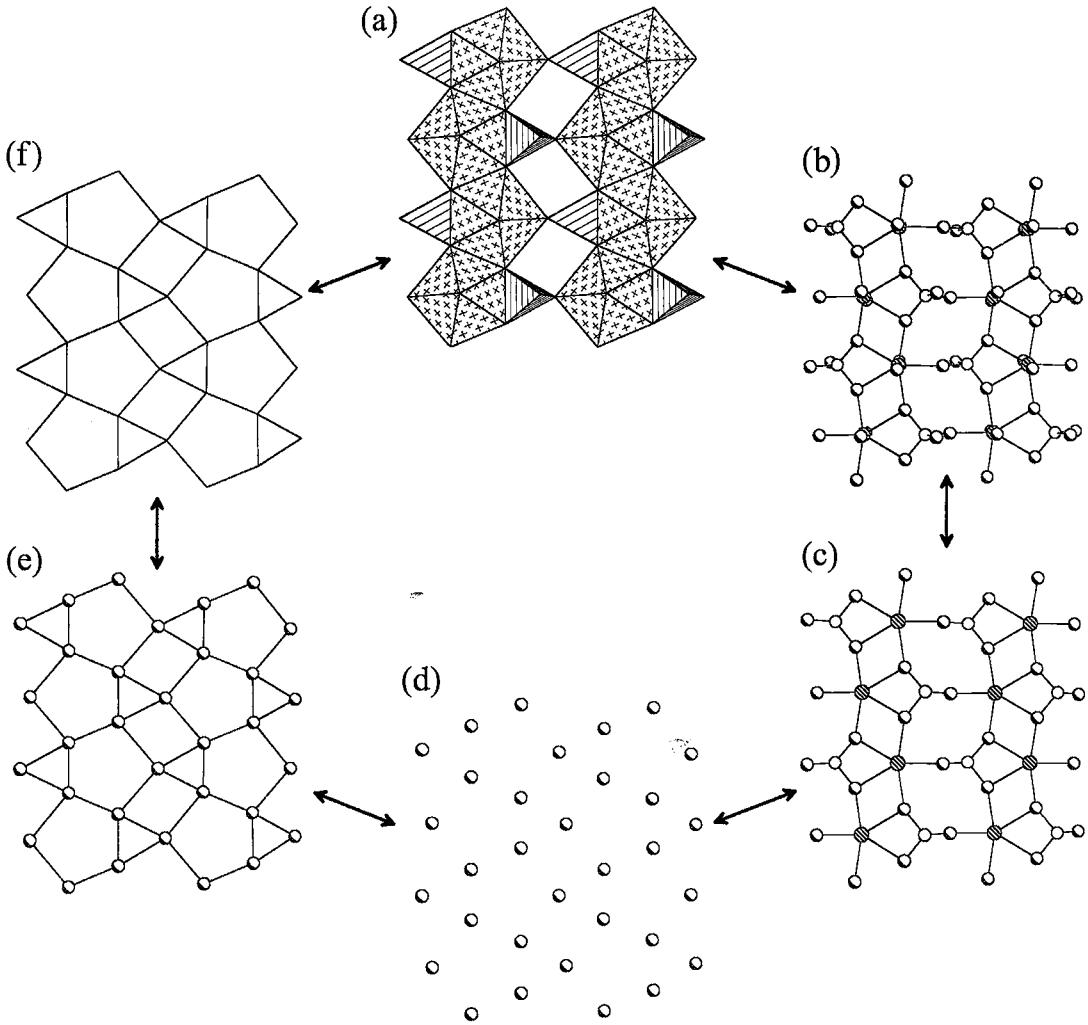

FIG. 2. The procedure for obtaining a sheet anion-topology that corresponds to a sheet of polyhedra. (a) The sheet of polyhedra. (b) A ball-and-stick representation of the sheet. (c) The sheet with all anions that are not bonded to two or more cations within the sheet, and are not an equatorial anion of a pyramid or bipyramid, removed. (d) The sheet with all cations, and cation–anion bonds, removed. (e) The sheet with anions connected. (f) The anion-topology of the sheet. The $Ur\phi_5$ polyhedra and $X\phi_4$ (X: unspecified cation) tetrahedra are shaded with crosses and parallel lines, respectively. Uranium atoms are shown as circles shaded with parallel lines, tetrahedrally coordinated cations are open circles, and anions are circles shaded in the lower-left corners.

joined by lines, with only those anions that may be realistically considered as part of the same coordination polyhedron being connected (*i.e.*, those anions separated by less than about 3.5 Å) (Fig. 2e). (4) Anions are removed from further consideration, leaving only a series of lines that represent the anion-topology (Fig. 2f). Note that the anion-topology does not contain any information about the cation population of the sheet from which the topology was derived.

All anion-topologies may be regarded as an orderly array of edge-sharing, space-filling polygons that possesses translational symmetry. Each polygon corresponds to a potential cation site in a particular (specific) population of that topology. For example, the center of a triangle may be populated by C, B or N, or by a cation in triangular–bipyramidal coordination, or the triangle may be the face of a tetrahedron, with the cation located above or below the center of the triangle, *etc.* A square may be populated by a cation in tetrahedral coordination, with all four anions bonded within the sheet, or by a cation in square-planar, square-pyramidal or octahedral coordination, *etc.* A specific filling of the cation sites associated with a topology is referred to as a *topology population.* Sheets of polyhedra, which in some cases seem to be very different, are commonly based upon the same underlying anion-topology, as demonstrated in Figure 3.

In the structural hierarchy presented here, all sheets are grouped according to the underlying anion-topology in the sheet. This approach is not only a reasonable and effective means of classification of these sheet structures, but it also provides the basis whereby new sheets may be predicted (Miller *et al.* 1996). In the following sections, each observed anion-topology in the sheet is considered in turn. In order to facilitate comparison, anion-topologies are loosely grouped according to the shapes of the polygons that they contain. We emphasize that this grouping is done primarily for the sake of convenience.

Anion-topologies with squares

There is only one way to construct an anion-topology that has only squares such that the anions of common edges of adjacent squares are coincident (Fig. 4a), and this topology is the basis of sheets found in twenty-two structures (Table 1). Only three topologically distinct sheets have this anion-topology, and the structures that contain them are grouped in Table 1 according to sheet type. This anion-topology is designated the autunite anion-topology.

The first group of structures in Table 1 is based upon a sheet in which one half of the squares of the anion-topology are populated by $Ur\phi_4$ polyhedra, such that there is only corner-sharing between adjacent $Ur\phi_4$ polyhedra, and the uranyl ions are perpendicular to the sheets (Fig. 4b). This sheet has the composition $(UO_2)O_2$ and occurs in seven structures (Table 1). In each structure, the sheets are either bonded together through interlayer cations (five structures) or hydrogen bonds between sheets (two structures).

The second group of structures in Table 1 is based upon a sheet that contains equal numbers of $Ur\phi_4$ polyhedra and $X^{5+}O_4$ tetrahedra. One half of the square sites of the anion-topology are populated; one quarter are populated with $Ur\phi_4$ polyhedra, and one quarter are populated with $X^{5+}O_4$ tetrahedra with all four anions contained within the sheet (Fig. 4c). The composition of this sheet is $(UO_2)(X^{5+}O_4)$, and it is found in fourteen structures (Table 1), with the tetrahedral sites occupied by X = P in eight and X = As in six. In twelve of the structures, the sheets are linked through interlayer cations and, in most cases, by hydrogen bonding. In two structures, the sheets are linked by hydrogen bonding only to interlayer H_2O groups.

The structure of $K_4[(UO_2)(PO_4)_2]$ contains twice as many PO_4 tetrahedra as $Ur\phi_4$ polyhedra (Fig. 4d). In this sheet, one quarter of the squares of the anion-topology (Fig. 4a) are populated by PO_4 tetrahedra and one eighth are populated by $Ur\phi_4$ polyhedra, giving a sheet with the composition $(UO_2)(PO_4)_2$. Each $Ur\phi_4$

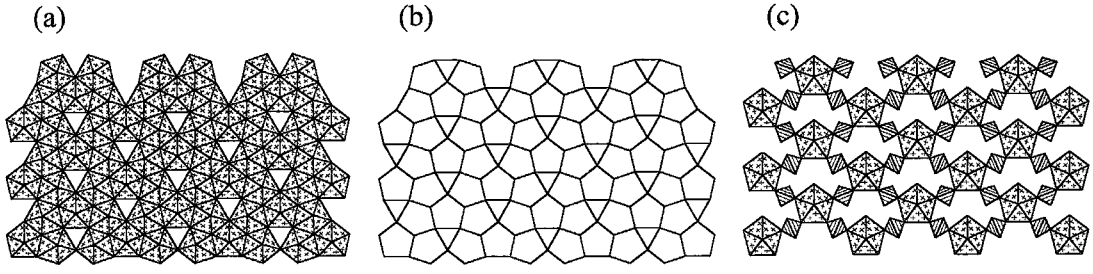

FIG. 3. Examples of sheets of polyhedra that have identical anion-topologies. (a) The sheet that occurs in the structure of protasite. (b) The protasite anion-topology. (c) The sheet that occurs in the structure of $Mg[(UO_2)(SO_4)_2](H_2O)_{11}$. Uranyl polyhedra are shaded with crosses, and tetrahedra are shaded with parallel lines.

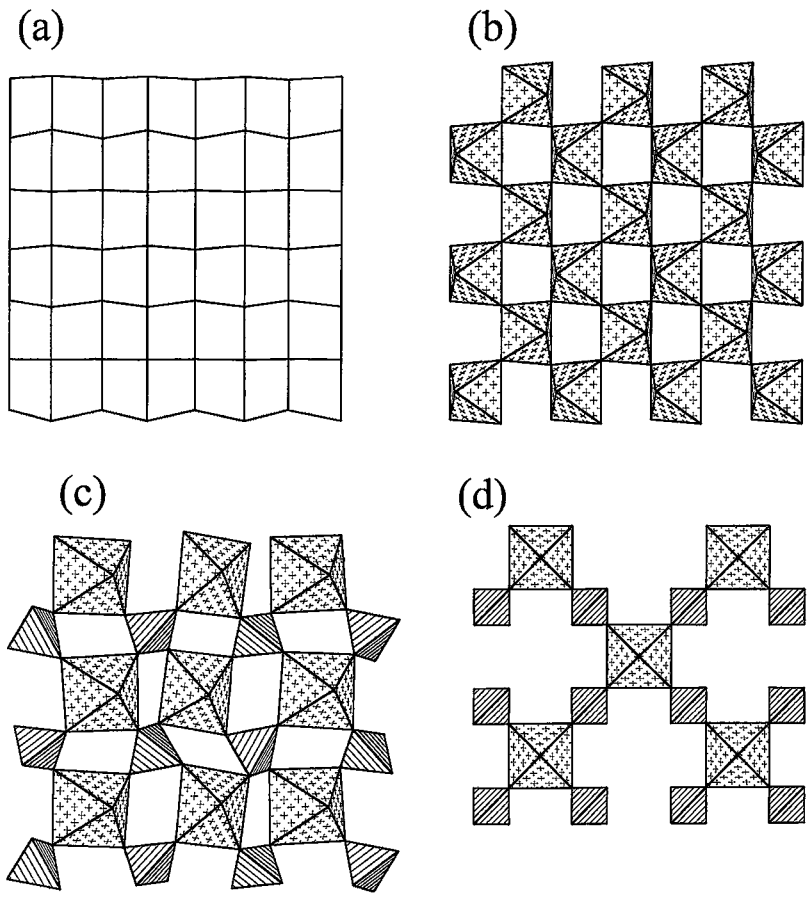

FIG. 4. Sheets based upon the anion-topology that contains only squares. The corresponding structures are listed in Table 1. Legend as in Figure 3.

polyhedron shares four of its corners with PO_4 tetrahedra, but each PO_4 tetrahedron is only connected to two $Ur\phi_4$ polyhedra. The sheets are connected through the interlayer K cations.

Anion-topologies with triangles and pentagons

Eleven structures contain sheets based on anion-topologies that contain only triangles and pentagons (Table 2). Only three unique anion-topologies occur in this group, and structures based on this sheet anion-topology are listed in Table 2.

Protasite anion-topology: The structure of protasite is based upon a sheet with the anion-topology shown in Figure 5b. This anion-topology contains a chain of edge-sharing pentagons, and each of these chains is separated by a chain containing pentagons and triangles, arranged so that each triangle shares an edge with one pentagon and a corner with another pentagon within the same chain (Fig. 5b). This chain of pentagons and triangles is referred to as an *arrowhead chain* by Miller *et al.* (1996) because the sharing of an edge between a pentagon and a triangle produces an arrowhead-like shape. In the protasite anion-topology, all arrowhead chains of pentagons and triangles are oriented such that the arrowheads point in the same direction (toward the bottom of the page in Fig. 5b).

Where all pentagons in the anion-topology are populated with $Ur\phi_5$ polyhedra, the sheet shown in Figure 5a results. This sheet, with composition $(UO_2)_3\phi_5$, is found in the structures of protasite, billietite (along with another sheet, see below), becquerelite, and α-U_3O_8 (Table 2). In the structures of protasite, billietite and becquerelite, the sheets are linked through intersheet cations and hydrogen bonds, but in α-U_3O_8, the sheets link directly by shared anions.

TABLE 1. STRUCTURES CONTAINING SHEETS BASED ON ANION TOPOLOGIES WITH SQUARES

Name	Fig.	Formula	S. G.	*a* (Å)	*b* (Å)	*c* (Å)	α (°)	β (°)	γ (°)	Ref.
	4b	$Li_2[(UO_2)O_2]$	*Pnma*	10.547	6.065	5.134				1
	4b	$Ba[(UO_2)O_2]$	*Pbcm*	5.744	8.136	8.237				2
	4b	$Sr[(UO_2)O_2]$	*Pbcm*	5.4896	7.9770	8.1297				3
	4b	γ-$[(UO_2)(OH)_2]$	$P2_1/c$	5.560	5.522	6.416		112.71		4
	4b	β-$[(UO_2)(OH)_2]$	*Pbca*	5.6438	6.2867	9.9372				5
	4b	β-$Na_2[(UO_2)O_2]$	*Pccn*	11.708	5.805	5.970				6
	4b	$Pb[(UO_2)O_2]$	*Pbcm*	5.536	7.968	8.212				7
meta-uranocircite	4c	$Ba[(UO_2)(PO_4)]_2(H_2O)_6$	$P2_1/a$	9.789	9.882	16.868			89.95	8
threadgoldite	4c	$Al[(UO_2)(PO_4)]_2(OH)(H_2O)_8$	*C2/c*	20.168	9.847	19.719		110.71		9
metatorbernite	4c	$Cu_{0.92}[(UO_2)(PO_4)]_2(H_2O)_8$	*P4/n*	6.972		17.277				10
meta-autunite	4c	$Ca[(UO_2)(PO_4)]_2(H_2O)_6$	*P4/nmm*	6.96		8.40				11
saleeite	4c	$Mg[(UO_2)(PO_4)]_2(H_2O)_{10}$	$P2_1/c$	6.951	19.947	9.896		135.17		12
	4c	$[(UO_2)H(PO_4)](H_2O)_4$	*P4/ncc*	6.995		17.491				13
	4c	$K[(UO_2)(PO_4)](D_2O)_3$	*P4/ncc*	6.99379		17.78397				14
	4c	$ND_4[(UO_2)(PO_4)](D_2O)_3$	*P4/ncc*	7.0221		18.0912				15
metazeunerite	4c	$Cu[(UO_2)(AsO_4)]_2(H_2O)_8$	$P4_2/nmc$	7.105		17.704				16
abernathyite	4c	$K[(UO_2)(AsO_4)](H_2O)_3$	*P4/ncc*	7.176		18.126				17
	4c	$NH_4[(UO_2)(AsO_4)](H_2O)_3$	*P4/ncc*	7.189		18.191				17
	4c	$KH_3O[(UO_2)(AsO_4)]_2(H_2O)_6$	*P4/ncc*	7.171		18.048				17
	4c	$[(UO_2)D(AsO_4)](D_2O)_4$	*P4/ncc*	7.1615		17.6390				18
	4c	$Li[(UO_2)(AsO_4)](D_2O)_4$	*P4/n*	7.0969		9.1903				19
	4d	$K_4[(UO_2)(PO_4)_2]$	$P4_2/nmc$	6.985		11.865				20

References: (1) Gebert *et al.* (1978), (2) Reis *et al.* (1976), (3) Loopstra & Rietveld (1969), (4) Siegel *et al.* (1972b), (5) Taylor & Bannister (1972), (6) Kovba (1971), (7) Cremers *et al.* (1986), (8) Khosrawan-Sazedj (1982a), (9) Khosrawan-Sazedj (1982b), (10) Stergiou *et al.* (1993), (11) Makarov & Ivanov (1960), (12) Miller & Taylor (1986), (13) Morosin (1978), (14) Fitch & Cole (1991), (15) Fitch & Fender (1983), (16) Hanic (1960), (17) Ross & Evans (1964), (18) Fitch *et al.* (1983) (19) Fitch *et al.* (1982), (20) Linde *et al.* (1980).

TABLE 2. STRUCTURES CONTAINING SHEETS BASED UPON ANION TOPOLOGIES CONTAINING TRIANGLES AND PENTAGONS

Name	Fig.	Formula	S. G.	*a* (Å)	*b* (Å)	*c* (Å)	α (°)	β (°)	γ (°)	Ref.
protasite	5a	$Ba[(UO_2)_3O_3(OH)_2](H_2O)_3$	*Pn*	12.2949	7.2206	6.9558		90.401		1
billietite	5a	$Ba[(UO_2)_3O_2(OH)_3]_2(H_2O)_4$	$Pbn2_1$	12.0720	30.167	7.1455				1
becquerelite	5a	$Ca[(UO_2)_3O_2(OH)_3]_2(H_2O)_8$	$Pn2_1a$	13.8378	12.3781	14.9238				1
	5a	α-U_3O_8	*C2mm*	6.716	11.960	4.147				2
	5c	$Mg[(UO_2)(SO_4)_2](H_2O)_{11}$	*C2/c*	11.334	7.715	21.709		102.22		3
	5c	$[(UO_2)(SO_4)_2]H_2(H_2O)_5$	*C2/c*	11.008	8.242	15.619		113.71		4
	5c	$K_2[UO_2(SO_4)_2](H_2O)_2$	*Pnma*	13.806	11.577	7.292				5
fourmarierite	5d	$Pb[(UO_2)_4O_3(OH)_4](H_2O)_4$	$Bb2_1m$	13.986	16.400	14.293				6
schoepite	5d	$[(UO_2)_8O_2(OH)_{12}](H_2O)_{12}$	$P2_1ca$	14.337	16.813	14.731				7
	5g	α-$Cs_2[(UO_2)_2O_3]$	*C2/m*	14.528	4.2638	7.605		112.		8
	5g	β-$Cs_2[(UO_2)_2O_3]$	*C2/m*	14. 615	4.3199	7.465		113.78		8

References: (1) Pagoaga *et al.* (1987), (2) Loopstra (1977), (3) Serezhkin *et al.* (1981b), (4) Alcock *et al.* (1982), (5) Niinistö *et al.* (1979), (6) Piret (1985), (7) Finch *et al.* (1996), (8) van Egmond (1976b).

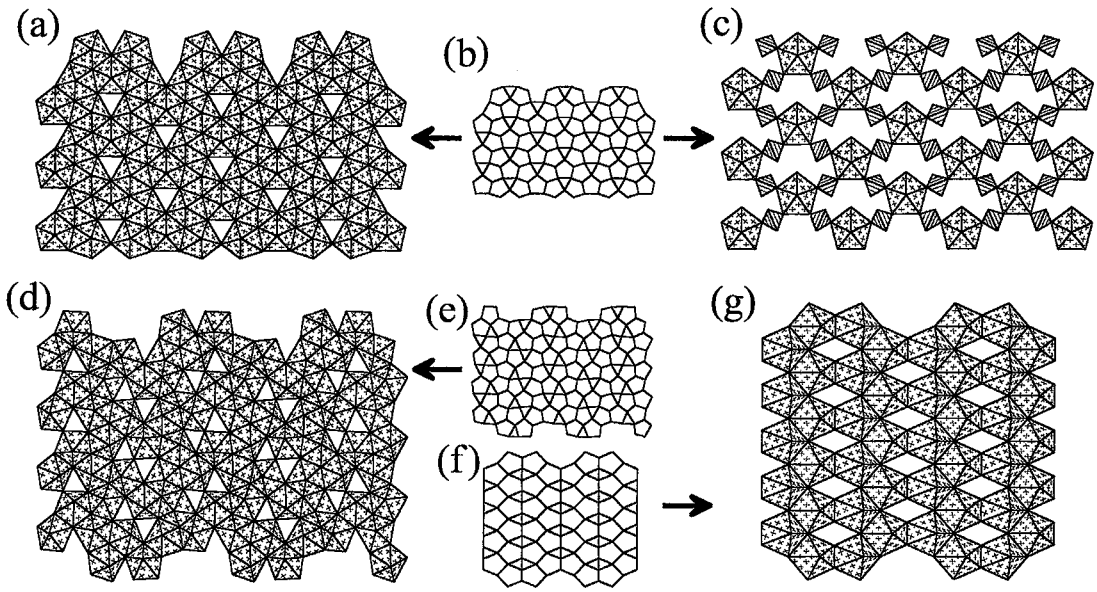

FIG. 5. Sheets based upon anion-topologies that contain triangles and pentagons. The corresponding structures are listed in Table 2. Legend as in Figure 3.

Where one half of the pentagons of the anion-topology shown in Figure 5b are filled with $Ur\phi_5$ polyhedra, and $S^{6+}O_4$ tetrahedra are inserted such that two anions of each tetrahedron are included in the sheet, with the tetrahedron edge corresponding to the shared edges of pentagons in the anion-topology, the sheet shown in Figure 5c results. This sheet has the composition $(UO_2)(SO_4)_2$ and is the basis of three structures (Table 2). In the structures of $Mg[(UO_2)(SO_4)_2](H_2O)_{11}$ and $K_2[(UO_2)(SO_4)_2](H_2O)_2$, the linkage between sheets is through intersheet cations and hydrogen bonds, and in $[(UO_2)(SO_4)_2]H_2(H_2O)_5$, the linkage between sheets occurs through hydrogen bonding only.

Fourmarierite anion-topology: The structures of fourmarierite and schoepite (Table 2) both contain sheets with the underlying anion-topology illustrated in Figure 5e. This anion-topology contains chains of edge-sharing pentagons that are separated by two adjacent arrowhead chains of pentagons and triangles, with the arrowheads of adjacent chains pointing in opposite directions (Fig. 5e). The sheet that occurs in the fourmarierite and schoepite structures (Fig. 5d) results by populating all pentagons in the anion-topology with $Ur\phi_5$ polyhedra, giving a sheet with composition $(UO_2)_4\phi_7$. In the structure of fourmarierite, adjacent sheets are linked through intersheet Pb cations and through hydrogen bonding, whereas the sheets in the structure of schoepite are connected *via* hydrogen bonding to intersheet H_2O groups only.

$Cs_2[(UO_2)_2O_3]$ anion-topology: The anion-topology shown in Figure 5f is the basis of the sheet that occurs in the α and β forms of $Cs_2[(UO_2)_2O_3]$ (Table 2). All pentagons in this novel anion-topology are populated by $Ur\phi_5$ polyhedra to give a sheet with composition $(UO_2)_2O_3$ (Fig. 5g). In both structures, the sheets are linked through the intersheet Cs cation. The α and β forms of $Cs_2[(UO_2)_2O_3]$ are similar; the two structures differ only in small atomic displacements associated with anion disorder (van Egmond 1976b).

Anion-topologies with triangles, squares and pentagons

Currently, forty-one structures are known to contain sheets with anion-topologies that contain only triangles, squares and pentagons. These structures are grouped on the basis of the underlying anion-topology in the sheet (Table 3). Within each group, structures that exhibit the same topology population are grouped. There are fifteen known distinct anion-topologies that contain only triangles, squares and pentagons. In the following sections, each of these topologies is discussed separately.

Uranophane anion-topology: The sheets of sixteen structures (Table 3) are based upon the anion-topology of the uranophane sheet (Fig. 6a). In this anion-topology, pentagons share edges to form parallel chains, and adjacent chains of pentagons are connected through chains of alternating edge-sharing triangles

TABLE 3. STRUCTURES CONTAINING SHEETS BASED UPON ANION TOPOLOGIES WITH TRIANGLES, SQUARES AND PENTAGONS

Name	Fig.	Formula	S. G.	*a* (Å)	*b* (Å)	*c* (Å)	α (°)	β (°)	γ (°)	Ref.
	6b	$Na[(UO_2)(BO_3)]$	*Pcam*	10.712	5.780	6.862				1
	6b	$Li[(UO_2)(BO_3)]$	$P2_1/c$	5.767	10.574	6.835		105.04		2
α-uranophane	6c	$Ca[(UO_2)(SiO_3OH)]_2(H_2O)_5$	$P2_1$	15.909	7.002	6.665		97.27		3
boltwoodite	6c	$K(H_3O)[(UO_2)(SiO_4)]$	$P2_1$	7.073	7.064	6.638		105.75		4
cuprosklodowskite	6c	$Cu[(UO_2)(SiO_3OH)]_2(H_2O)_6$	$P\bar{1}$	7.052	9.267	6.655	109.23	89.84	110.01	5
sklodowskite	6c	$Mg[(UO_2)(SiO_3OH)]_2(H_2O)_6$	$C2/m$	17.382	7.047	6.610		105.9		6
kasolite	6c	$Pb[(UO_2)(SiO_4)](H_2O)$	$P2_1/c$	6.704	6.932	13.252		104.22		7
	6c	$Mg[(UO_2)(AsO_4)]_2(H_2O)_4$	$C2/m$	18.207	7.062	6.661		99.65		8
β-uranophane	6d	$Ca[(UO_2)(SiO_3OH)]_2(H_2O)_5$	$P2_1/a$	13.966	15.443	6.632		91.38		9
ulrichite	6e	$Cu[Ca(UO_2)(PO_4)_2](H_2O)_4$	$C2/m$	12.79	6.85	13.02		91.03		10
	6f	$Na_{5.5}(UO_2)_3(H_{0.5}PO_4)(PO_4)_3$	$P1$	6.675	6.922	10.732	83.96	82.29	89.44	11
	6g	$K_2[(UO_2)_2O_3]$	$P2_1$	6.931	7.690	6.984		109.69		12
	6h	$[H_2(UO_2)_3O_4]$	$P\bar{1}$	6.802	7.417	5.556	108.5	125.5	88.2	13
	6i	$[(UO_2)(CuO_4)]$	$P\bar{1}$	6.516	7.614	5.615	109.464	125.18	89.993	14
schmitterite	6j	$[(UO_2)(TeO_3)]$	$Pca2_1$	10.161	5.363	7.862				15
	6k	$K[(UO_2)(NbO_4)]$	*Pcab*	7.579	11.321	15.259				16
francevillite	7a	$Ba_{0.96}Pb_{0.04}[(UO_2)_2(V_2O_8)](H_2O)_5$	*Pcan*	10.419	8.510	16.763				17
curienite	7a	$Pb[(UO_2)_2(V_2O_8)](H_2O)_5$	*Pcan*	10.40	8.45	16.34				18
	7a	$K_2[(UO_2)_2(V_2O_8)]$	$P2_1/a$	10.47	8.41	6.59		103.8		19
sengierite	7a	$Cu_2[(UO_2)_2(V_2O_8)](OH)_2(H_2O)_6$	$P2_1/a$	10.599	8.093	10.085		103.42		20
	7a	$Ni[(UO_2)_2(V_2O_8)](H_2O)_4$	*Pnam*	10.60	8.25	15.12				21
	7a	$Cs_2[(UO_2)_2(V_2O_8)]$	$P2_1/a$	10.521	8.436	7.308		106.08		22
	7a	$Cs_2[(UO_2)_2(Nb_2O_8)]$	$P2_1/c$	7.430	8.700	10.668		105.08		23
	7d	$β\text{-}U_3O_8$	*Cmcm*	7.069	11.445	8.303				24
billietite	7d	$Ba[(UO_2)_3O_2(OH)_3]_2(H_2O)_4$	$Pbn2_1$	12.0720	30.167	7.1455				25
iriginite	7e	$[(UO_2)(MoO_3OH)_2(H_2O)](H_2O)$	$Pca2_1$	12.77	6.715	11.53				26
	7g	$[Ca(UO_2)MoO_4O_{14}]$	$P\bar{1}$	13.239	6.651	8.236	90.00	90.38	120.16	27
sayrite	7h	$Pb_2[(UO_2)_5O_6(OH)_2](H_2O)_4$	$P2_1/c$	10.704	6.960	14.533		116.81		28
	7h	$K_2[(UO_2)_5O_8](UO_2)_2$	*Pbam*	6.945	19.533	7.215				29
	7k	$[Pb_3(UO_2)_{11}O_{14}]$	*Pmmn*	28.459	8.379	6.7650				30
	7k	$[Sr_3(UO_2)_{11}O_{14}]$	*Pmmn*	28.508	8.380	6.7333				31
	7l	$K[(UO_2)(CrO_4)(OH)](H_2O)_{1.5}$	$P2_1/c$	13.292	9.477	13.137		104.12		32
	7o	$Cs[(UO_2)(PO_3)_3]$	$P2_1/n$	6.988	10.838	13.309		104.25		33
curite	7p	$Pb_3[(UO_2)_8O_8(OH)_6](H_2O)_3$	*Pnam*	12.551	13.003	8.390				34
	7s	$Cs_4[(UO_2)_5O_7]$	*Pbcn*	18.776	7.070	14.958				35
vandenbrandeite	7t	$[(UO_2)Cu(OH)_4]$	$P\bar{1}$	7.855	5.449	6.089	91.44	101.90	89.2	36
zippeite	7w	$K[(UO_2)_2(SO_4)(OH)_3](H_2O)$	$C2/c$	8.755	13.987	17.730		104.13		37
	7x	$Cs_2[(UO_2)_2(SO_4)_3]$	$P\bar{4}21$	9.62		8.13				38
	7aa	$(NH_4)_2[(UO_2)(SO_4)_2(H_2O)](H_2O)$	$P2_1/c$	7.783	7.403	20.918		102.25		39
	7ab	$[Mg(UO_2)(B_2O_5)]$	*Pcam*	9.747	7.315	7.911				40
	7ae	$K_2[(UO_2)(MoO_4)]$	$P2_1/c$	12.269	13.468	12.857		95.08		41

References: (1) Gasperin (1988), (2) Gasperin (1990), (3) Ginderow (1988), (4) Stohl & Smith (1981), (5) Rosenzweig & Ryan (1975), (6) Ryan & Rosenzweig (1977), (7) Rosenzweig & Ryan (1977a), (8) Bachet *et al.* (1991), (9) Viswanathan & Harneit (1986), (10) Birch *et al.* (1988), (11) Gorbunova *et al.* (1980), (12) Saine (1989), (13) Siegel *et al.* (1972a), (14) Dickens *et al.* (1993), (15) Meunier & Galy (1973), (16) Gasperin (1987b), (17) Mereiter (1986e), (18) Borene & Cesbron (1971), (19) Appleman & Evans (1965), (20) Piret *et al.* (1980), (21) Borene & Cesbron (1970), (22) Dickens *et al.* (1992), (23) Gasperin (1987c), (24) Loopstra (1970), (25) Pagoaga *et al.* (1987), (26) Serezhkin *et al.* (1973), (27) Lee & Jaulmes (1987), (28) Piret *et al.* (1983), (29) Kovba (1972a), (30) Ijdo (1993a), (31) Cordfunke *et al.* (1991), (32) Serezhkina *et al.* (1990), (33) Linde *et al.* (1978), (34) Taylor *et al.* (1981), (35) van Egmond (1976a), (36) Rosenzweig & Ryan (1977b), (37) Vochten *et al.* (1995), (38) Ross & Evans (1960), (39) Niinistö *et al.* (1978), (40) Gasperin (1987a), (41) Sadikov *et al.* (1988).

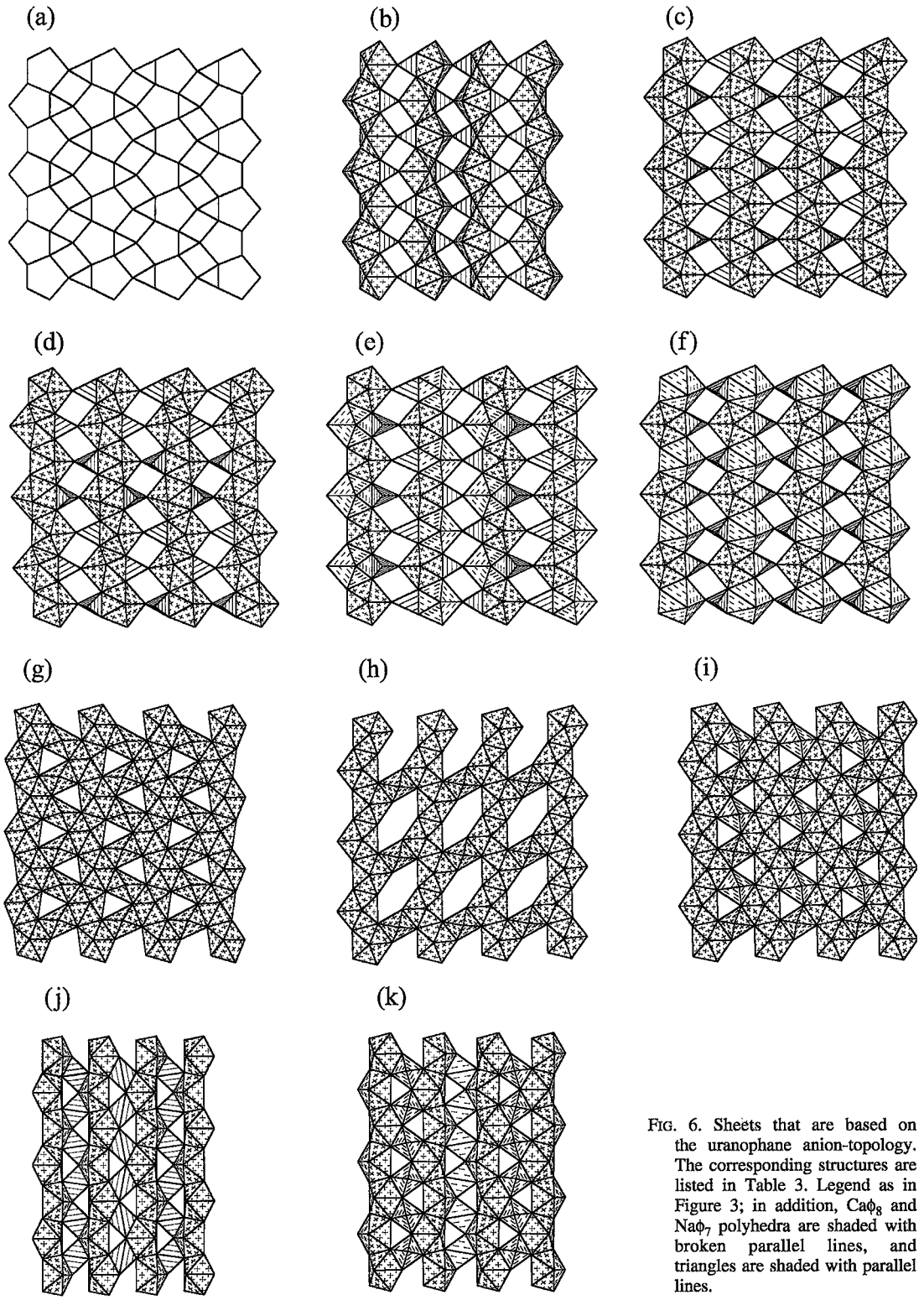

FIG. 6. Sheets that are based on the uranophane anion-topology. The corresponding structures are listed in Table 3. Legend as in Figure 3; in addition, $Ca\phi_8$ and $Na\phi_7$ polyhedra are shaded with broken parallel lines, and triangles are shaded with parallel lines.

and squares. Alternatively, this anion-topology may be described as containing arrowhead chains of pentagons and triangles (the chains are horizontal in Fig. 6a) that are separated by isolated squares (the squares are equivalent to the R-chains of Miller *et al.* 1996). Note that the arrowheads of adjacent arrowhead chains point in opposite directions (Fig. 6a). There are ten distinct ways in which this anion-topology is populated to form sheets (Fig. 6), which are the bases of the sixteen structures. Notably, there are no examples of this topology in which both the triangles and squares are populated.

First, consider sheets with occupied triangles. Populating all pentagons of the uranophane anion-topology with $Ur\phi_5$ polyhedra and each triangle with a BO_3 triangle results in a sheet with composition $(UO_2)(BO_3)$ (Fig. 6b). This sheet is the basis of the structures of $Na[(UO_2)(BO_3)]$ and $Li[(UO_2)(BO_3)]$; in $Na[(UO_2)(BO_3)]$, the sheets are stacked so as to provide octahedral coordination for the interlayer Na, whereas in $Li[(UO_2)(BO_3)]$, the interlayer Li is tetrahedrally coordinated. The considerable mismatch of the ideal edge-lengths of the $Ur\phi_5$ polyhedron (edge length $\approx$ 2.75 Å) and the BO_3 triangle (edge length $\approx$ 2.37 Å) is accommodated by a modulation of the sheet, such that the $Ur\phi_5$ polyhedra tilt in alternating directions in adjacent chains of edge-sharing pentagons (Fig. 6b).

Several structures are based upon sheets in which each pentagon of the uranophane anion-topology is populated by a $Ur\phi_5$ polyhedron, and triangles are the faces of tetrahedra (Figs. 6c, d). The sheets shown in Figures 6c and 6d differ in the orientation of adjacent tetrahedra. Going along the chain of edge-sharing triangles and squares in the anion-topology, the apices of adjacent tetrahedra alternate up (U) and down (D) with the sequence UDUDUD in sheet 6c, and UUDDUU in sheet 6d. In both cases, the apices of all tetrahedra in an arrowhead chain of pentagons and triangles point in the same direction. Both sheets have the composition $(UO_2)(X\phi_4)$, where X is the tetrahedrally coordinated cation. The sheet shown in Figure 6c is the basis of several structures. In the structures of α-uranophane, boltwoodite, cuprosklodowskite, sklodowskite and kasolite, the tetrahedra are $Si\phi_4$, and in $Mg[(UO_2)(AsO_4)]_2(H_2O)_4$, the tetrahedra are AsO_4. The sheet shown in Figure 6d occurs only in the structure of β-uranophane, where the tetrahedra are $Si\phi_4$. In each of these structures, sheets are linked through intersheet polyhedra involving low-valence cations and hydrogen bonds.

The structure of ulrichite contains sheets in which only half of the pentagons of the uranophane anion-topology are populated by $Ur\phi_5$ polyhedra, whereas the other pentagons are the locations of $Ca\phi_8$ polyhedra (Fig. 6e). The PO_4 tetrahedra are located at the triangles in the anion-topology. One type of PO_4 tetrahedron shares an edge with a $Ur\phi_5$ polyhedron and also an edge with the $Ca\phi_8$ polyhedron in the adjacent chain of edge-sharing pentagons. This tetrahedron is unusual because all four of its anions are bonded within the sheet. However, as the edge shared with the $Ca\phi_8$ polyhedron is perpendicular to the sheet, the tetrahedron projects as a triangle. The other type of PO_4 tetrahedron shares an edge with a $Ca\phi_8$ polyhedron and a corner with the adjacent $Ur\phi_5$ polyhedron. These two types of PO_4 tetrahedra occur in equal numbers and are distributed such that only one occurs in each chain of edge-sharing triangles and squares of the underlying anion-topology. In the arrowhead chains of pentagons and triangles, the pentagons are alternately populated with $Ur\phi_5$ and $Ca\phi_8$ polyhedra. There are two distinct types of arrowhead chains; in one, the apices of tetrahedra all point in the same direction, whereas in the other, they alternate up and down (Fig. 6e). The composition of the resulting sheet is $Ca(UO_2)(PO_4)_2$. Intersheet bonding occurs through Cu^{2+} positions (which are disordered) and hydrogen bonds.

The structure of $Na_{5.5}(UO_2)_3(H_{0.5}PO_4)(PO_4)_3$ contains the sheet shown in Figure 6f. This sheet is obtained from the anion-topology shown in Figure 6a by populating half of the pentagons with $Ur\phi_5$ polyhedra and half with $Na\phi_7$ pentagonal bipyramids, such that the $Ur\phi_5$ and $Na\phi_7$ polyhedra alternate along the chain of edge-sharing pentagons. There are two distinct arrowhead chains of pentagons and triangles; one contains $Ur\phi_5$ polyhedra, and the other contains $Na\phi_7$ pentagonal bipyramids. Each triangle is populated with a PO_4 tetrahedron, with the apices of all tetrahedra of a given sheet pointing in the same direction. In the structure, two of these sheets occur such that the apices of PO_4 tetrahedra point toward the other sheet. A $Ur\phi_4$ polyhedron is located between the two sheets, and the equatorial anions of the $Ur\phi_4$ polyhedra are the apical anions of two PO_4 tetrahedra in either sheet. The resulting double sheets are connected through interlayer Na cations to form the structure.

Now consider sheets with occupied squares. A number of sheets that are based upon the uranophane anion-topology have the square sites populated. In each of these cases, the pentagons in the anion-topology are all populated by $Ur\phi_5$ polyhedra. Populating each square with a $Ur\phi_4$ polyhedron results in a sheet with composition $(UO_2)_2O_3$ (Fig. 6g). This sheet is the basis of the structure of $K_2[(UO_2)_2O_3]$, where sheets are linked through the intersheet K cation. If only half the squares are populated by $Ur\phi_4$ polyhedra, the sheet shown in Figure 6h results. This sheet, of composition $(UO_2)_3\phi_6$, is the basis of the structure of $[H_2(UO_2)_3O_4]$. In this structure, the linear uranyl ions of the $Ur\phi_4$ polyhedra lie *within* the sheets, rather than perpendicular to them. This unusual arrangement is necessary because adjacent sheets are linked by sharing anions, rather than through an interlayer cation. One O_{Ur} atom of each $Ur\phi_5$ polyhedron is an equatorial oxygen

atom of a $Ur\phi_4$ polyhedron in the adjacent sheet.

Populating half of the square sites with $Cu^{2+}O_6$ octahedra and half with $Ur\phi_4$ polyhedra gives the sheet shown in Figure 6i. This sheet, with $[(UO_2)_3CuO_8]$ composition, occurs exclusively in the structure of $[(UO_2)_3(CuO_4)]$, where the sheets are linked by sharing anions. As observed in the structure of $[H_2(UO_2)_3O_4]$ above, this connectivity is possible because the uranyl ion of the $Ur\phi_4$ polyhedron lies within the sheet. The O_{Ur} of the $Ur\phi_5$ polyhedra are also the apical oxygen

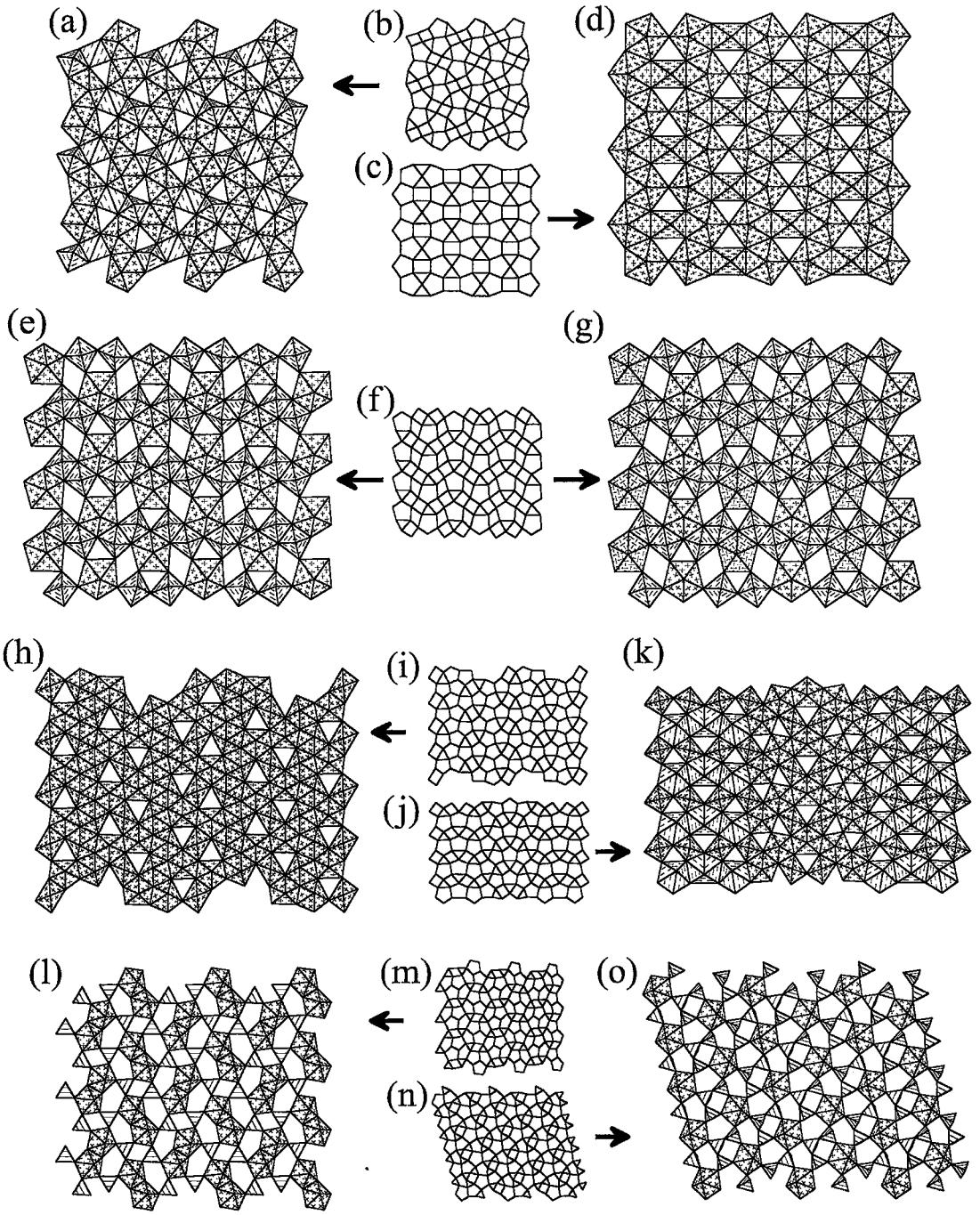

atoms of the (4 + 2)-distorted $Cu^{2+}O_6$ octahedron, and equatorial anions of the $Ur\phi_4$ polyhedra in adjacent sheets.

The structure of schmitterite is based upon a sheet with the square sites occupied by $Te^{4+}\phi_4$ polyhedra (Fig. 6j), giving a sheet of composition $(UO_2)(TeO_3)$. Owing to the lone pair of electrons on the Te^{4+} cation, all four anions of the coordination polyhedron occur on one side of the cation. Van der Waals forces as well as weak Te–O interactions over distances

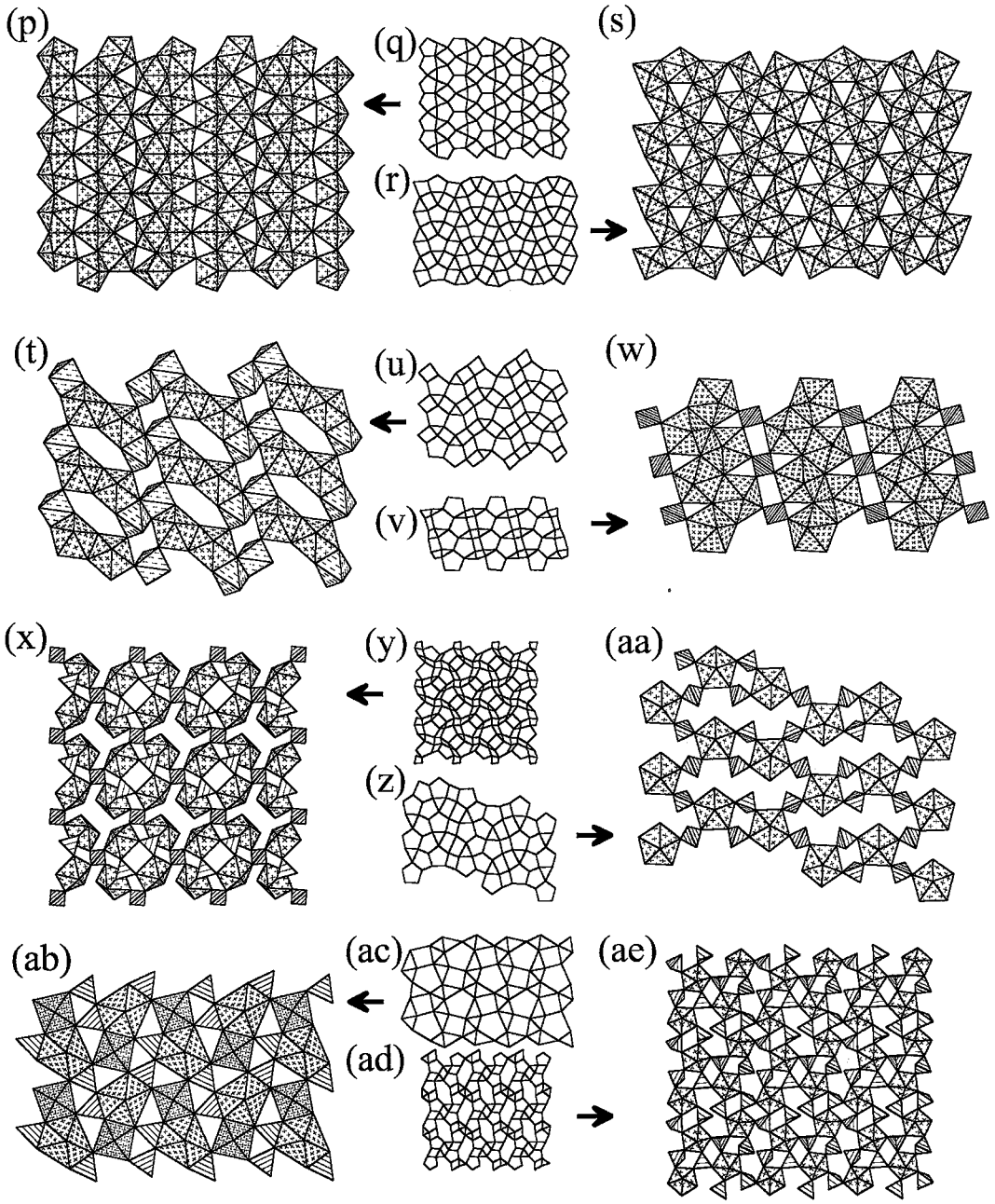

FIG. 7. Sheets based upon anion-topologies that contain triangles, squares and pentagons. The corresponding structures are listed in Table 3. Legend as in Figure 3 except that non-U^{6+} pentagonal bipyramids, octahedra and square pyramids are shaded with broken parallel lines.

exceeding 3.1 Å bond sheets together.

In the structure of $K[(UO_2)(NbO_4)]$, the squares in the anion-topology are populated by NbO_5 square pyramids (Fig. 6k), giving a sheet with $(UO_2)(NbO_4)$ composition. The apical anions of the NbO_5 square pyramids along each chain of edge-sharing triangles and squares in the anion-topology either point all up or all down. The sheets are linked through the intersheet K cations.

Francevillite anion-topology: The structure of francevillite contains sheets with the anion-topology shown in Figure 7b. In this anion-topology, edge-sharing dimers of pentagons share corners, creating both triangles and squares (Fig. 7b). There is only one observed population of this anion-topology (Fig. 7a), and the structures of seven phases are based upon it (Table 3). All pentagons in the anion-topology are populated by $Ur\phi_5$ polyhedra, and all triangles are empty. The anion-topology contains an edge-sharing dimer of squares, and in this sheet each is populated by $X^{5+}O_5$ square pyramids. The square in the anion-topology is the base of the square pyramid, and apical anions point up and down in each X_2O_8 dimer (Fig. 7a). The resulting sheet has the composition $(UO_2)_2(X_2O_8)$. In the structures of francevillite, curienite, $K_2[(UO_2)_2(V_2O_8)]$, sengeirite, $Ni[(UO_2)_2(V_2O_8)](H_2O)_4$ and $Cs_2[(UO_2)_2(V_2O_8)]$, the square pyramidal site is occupied by V^{5+}, and in $Cs_2[(UO_2)_2(Nb_2O_8)]$, it is occupied by Nb^{5+}. In each structure, the sheets are bonded together through interlayer cations and, in some cases, through hydrogen bonds as well.

β-U_3O_8 anion-topology: The structure of β-U_3O_8 contains a sheet with the anion-topology shown in Figure 7c. This anion-topology contains parallel, chains of edge-sharing pentagons. Each chain is separated by a chain that contains triangles and squares, and there are two triangles for each square. Note that this anion-topology also contains arrowhead chains of pentagons and triangles that are diagonal in Figure 7c. The arrowhead chains occur in pairs, with the arrowheads of adjacent chains pointing in opposite directions, and the pairs of arrowhead chains are separated by isolated squares (R-chains).

Only one sheet is known to have this anion-topology (Fig. 7d). Each pentagon of the anion-topology is populated by a $Ur\phi_5$ polyhedron, each square by a $Ur\phi_4$ polyhedron, and the triangles are empty. This sheet, with composition $(UO_2)_3\phi_5$, is found in the structures of β-U_3O_8 and billietite (along with a second sheet, see below) (Table 3). In billietite, the sheets are bonded together through the interlayer Ba cation and through hydrogen bonds to interlayer H_2O groups. In the structure of β-U_3O_8, there are no interlayer cations; the sheets are connected by sharing oxygen atoms.

The structure of billietite is exceptional because it contains two different sheets, each of which is based upon a slightly different anion-topology. One sheet is based upon the β-U_3O_8 anion-topology (Fig. 7c), whereas the other sheet has the protasite anion-topology (Fig. 5b). Comparison of these two anion-topologies shows that they both have parallel chains of edge-sharing pentagons. The anion-topologies differ in the manner in which these chains are separated; in the β-U_3O_8 anion-topology (Fig. 7c), the chains are separated by chains of squares and triangles, whereas in the protasite anion-topology (Fig. 5b), the chains are separated by chains composed of pentagons and triangles. Distortion of the pentagons in this chain in the protasite anion-topology such that two edges parallel the chain length results in transformation of the pentagon into a square–triangle combination, and the β-U_3O_8 anion-topology results. Thus although these two anion-topologies are distinct, they are related by relatively small displacements of two anions.

Iriginite anion-topology: The sheet upon which the structure of iriginite is based has the anion-topology shown in Figure 7f. This topology contains chains of pentagons and squares that share edges and zigzag chains of edge-sharing squares and triangles; both chains are horizontal in Figure 7f. Alternatively, the anion-topology can be described as a combination of arrowhead chains of pentagons and triangles (vertical in Fig. 7f) separated by zigzag chains of edge-sharing squares [the zigzag chains correspond to the triple R-chains of Miller *et al.* (1996)]. Only one population of the iriginite anion-topology is observed, and two structures are based on sheets with this population (Table 3). In the structure of iriginite, each pentagon of the underlying anion-topology is populated by a $Ur\phi_5$ polyhedron; two-thirds of the squares are populated with $Mo^{6+}O_6$ octahedra that occur as edge-sharing dimers, and the triangles as well as the squares that are part of the chains of edge-sharing pentagons and squares are empty (Fig. 7e). The sheets, with composition $(UO_2)(MoO_4)_2O$, are bonded together through hydrogen bonding to intersheet H_2O groups. The sheet in the structure of $[Ca(UO_2)Mo_4O_{14}]$ is identical to that of iriginite, except that every second pentagon along the chain of edge-sharing pentagons and squares of the anion-topology is populated by a $Ca\phi_7$ pentagonal bipyramid, rather than by a $Ur\phi_5$ polyhedron, giving a sheet with composition $Ca(UO_2)Mo_4O_{18}$ (Fig. 7g). In the structure of $Ca(UO_2)Mo_4O_{14}$, there are no intersheet species; sheets are connected by sharing anions. The O_{Ur} atoms of the $Ur\phi_5$ polyhedron are the apical anions of the $Ca\phi_7$ pentagonal bipyramids in sheets on either side, and $Mo^{6+}O_6$ octahedra share non-sheet anions.

Sayrite anion-topology: The anion-topology of the sheet that occurs in the structure of sayrite is shown in Figure 7i. This is a complex topology that contains

chains of edge-sharing pentagons separated by two arrowhead chains of pentagons and triangles that are in turn separated by isolated squares. One population of this anion-topology is known, and the resulting sheet occurs in two structures (Table 3).

Both the structures of sayrite and $K_2[(UO_2)_5O_8](UO_2)_2$ are based on the sheet shown in Figure 7h. Each pentagon of the underlying anion-topology (Fig. 7i) is populated by a $Ur\phi_5$ polyhedron, each square with a $Ur\phi_4$ polyhedron, and the triangles are empty. This gives a sheet with composition $(UO_2)_5\phi_8$. In the structure of sayrite, the sheets are linked through interlayer Pb cations and through hydrogen bonding. In the structure of $K_2[(UO_2)_5O_8](UO_2)_2$, the sheets are linked though interlayer K cations and a dimer of *face-sharing* $Ur\phi_5$ polyhedra, where only one of the two U positions in the dimer may be occupied on a local scale.

$Pb_3(UO_2)_{11}O_{14}$ anion-topology: The structure of $Pb_3(UO_2)_{11}O_{14}$ is based upon a sheet with the underlying anion-topology shown in Figure 7j. This anion-topology contains several distinct arrowhead chains of pentagons and triangles, 75% of which are separated by isolated squares (R-chains) (Fig. 7j). Only one population of this anion-topology is known, and it occurs in two structures (Table 3).

The structures of $Pb_3(UO_2)_{11}O_{14}$ and $Sr_3(UO_2)_{11}O_{14}$ both contain the sheet shown in Figure 7k, which is based on the anion-topology shown in Figure 7j. In the $Pb_3(UO_2)_{11}O_{14}$ sheet, all squares in the anion-topology (Fig. 7j) are populated by $Ur\phi_4$ polyhedra, and the triangles are empty. The pentagons of the anion-topology are populated both by $Ur\phi_5$ polyhedra and by $Pb\phi_7$ pentagonal bipyramids (Fig. 7k). In each arrowhead chain of pentagons and triangles, pentagons are either all populated by $Ur\phi_5$ polyhedra or all populated by $Pb\phi_7$ pentagonal bipyramids. Groups of three arrowhead chains containing $Pb\phi_7$ pentagonal bipyramids are separated by five arrowhead chains that contain $Ur\phi_5$ polyhedra (Fig. 7k).

The structure of $Sr_3(UO_2)_{11}O_{14}$ is based upon an identical sheet, except that the pentagons occupied by $Pb\phi_7$ pentagonal bipyramids in $Pb_3(UO_2)_{11}O_{14}$ are here occupied by $Sr\phi_7$ pentagonal bipyramids. The sheets are bonded directly together by sharing anions. In the structures of $Pb_3(UO_2)_{11}O_{14}$ and $Sr_3(UO_2)_{11}O_{14}$, the uranyl ions of the four unique $Ur\phi_5$ polyhedra are oriented perpendicular to the sheet, but in the two $Ur\phi_4$ polyhedra, the uranyl ions lie within the sheet. The sheets are stacked so that the O_{Ur} atoms of two of the $Ur\phi_5$ polyhedra are the apical atoms of oxygen of $(Pb,Sr)\phi_7$ pentagonal bipyramids in adjacent sheets, and the O_{Ur} atoms of the other two $Ur\phi_5$ polyhedra are equatorial anions in $Ur\phi_5$ polyhedra in adjacent sheets.

Other anion-topologies: Ten structures are based upon sheets that have unique anion-topologies that contain triangles, squares and pentagons.

Sheets with both triangles and pentagons populated occur in several structures. The structures of $K[(UO_2)(CrO_4)(OH)](H_2O)_{1.5}$ and $Cs[(UO_2)(PO_3)_3]$ are based on sheets with the anion-topologies shown in Figures 7m and 7n, respectively. The structure of $K[(UO_2)(CrO_4)(OH)](H_2O)_{1.5}$ contains sheets with edge-sharing dimers of $Ur\phi_5$ polyhedra, each of which shares corners with six $Cr^{6+}O_4$ tetrahedra (Fig. 7*l*), giving a sheet with composition $(UO_2)(CrO_4)(OH)$. Bonding between sheets occurs through the interlayer K cations and hydrogen bonding. The sheets of the $Cs[(UO_2)(PO_3)_3]$ structure contain $Ur\phi_5$ polyhedra that share corners with five PO_4 tetrahedra, giving a sheet of composition $(UO_2)(PO_3)_3$ (Fig. 7o). The sheets are connected through the interlayer Cs cations.

Sheets in which both squares and pentagons are occupied occur in several structures. The structures of curite, $Cs_4[(UO_2)_5O_7]$, vandenbrandeite and zippeite are based on sheets with the anion-topologies shown in Figures 7q, r, u, v. Only one population of each of these anion-topologies occurs, and each population is known from only one structure.

The structure of curite is based upon the sheet shown in Figure 7p. All pentagons and squares of the corresponding anion-topology of the sheet (Fig. 7q) are populated by $Ur\phi_5$ and $Ur\phi_4$ polyhedra, respectively. The sheets are linked through the interlayer Pb cations and through hydrogen bonds.

The sheet that occurs in the structure of $Cs_4[(UO_2)_5O_7]$ contains both $Ur\phi_5$ and $Ur\phi_4$ polyhedra (Fig. 7s), with the anion-topology shown in Figure 7r. Each $Ur\phi_5$ polyhedron shares four of its edges with $Ur\phi_4$ polyhedra, whereas each $Ur\phi_4$ polyhedron shares an edge with both a $Ur\phi_5$ and a $Ur\phi_4$ polyhedron. Edge-sharing between $Ur\phi_4$ polyhedra in a structure is exceptionally rare; the only other example is in the structure of $K_8[(UO_2)_2O_4]$, which contains isolated edge-sharing $Ur\phi_4$ dimers (see below, Fig. 12h). In the structure of $Cs_4[(UO_2)_5O_7]$, the sheets are linked through the interlayer Cs cations.

The structure of vandenbrandeite contains a sheet that has dimers of edge-sharing $Ur\phi_5$ polyhedra and dimers of edge-sharing $Cu\phi_5$ square pyramids (Fig. 7t), and the anion-topology is shown in Figure 7u. This anion-topology contains arrowhead chains of pentagons and triangles that are separated alternately by isolated squares (R-chains) and zigzag chains of edge-sharing squares (triple R-chains). The arrowheads of adjacent arrowhead-chains point in opposite directions. In each dimer of $Cu\phi_5$ square pyramids, the apices of the two square pyramids point in opposite directions, and the apical anion of the square pyramid is also the O_{Ur} atom in a $Ur\phi_5$ polyhedron of an adjacent sheet.

The structure of zippeite is based upon the sheet shown in Figure 7w, which has the anion-topology shown in Figure 7v. The zippeite anion-topology is

similar to the $Cs_2[(UO_2)_2O_3]$ anion-topology (Fig. 5f). Both anion-topologies contain identical chains of edge-sharing pentagons. In the $Cs_2[(UO_2)_2O_3]$ anion-topology, the chains of pentagons share edges with adjacent chains (Fig. 5f), whereas in the zippeite anion-topology (Fig. 7v), the chains are connected by sharing edges with a chain of edge-sharing squares. The sheets in the structure of zippeite are connected through interlayer K cations and hydrogen bonds to interlayer H_2O groups.

The structure of $Cs_2[(UO_2)_2(SO_4)_3]$ contains complex sheets (Fig. 7x) that have the anion-topology shown in Figure 7y. Each pentagon in the anion-topology is populated with a $Ur\phi_5$ polyhedron, and $S^{6+}O_4$ tetrahedra are located in triangles and at squares in the anion-topology. The sheets are linked through the intersheet Cs cations.

The sheet that is the basis of the structure of $(NH_4)_2[UO_2(SO_4)_2(H_2O)](H_2O)$ is shown in Figure 7aa. The corresponding anion-topology (Fig. 7z) contains arrowhead chains of pentagons and triangles. These chains are separated from similar chains on either side by chains of edge-sharing pentagons on one side and zigzag chains of edge-sharing squares (triple R-chains) on the other. The sheet is derived by populating only the pentagons in the arrowhead chain of pentagons and triangles with $Ur\phi_5$ polyhedra and inserting $S^{6+}O_4$ tetrahedra such that a tetrahedron edge joins pentagons of adjacent chains (Fig. 7aa). The sheets are connected through hydrogen bonds to intersheet NH_4 and H_2O groups.

The structure of $[Mg(UO_2)(B_2O_5)]$ contains the sheet shown in Figure 7ab, which has the anion-topology shown in Figure 7ac. The sheet is derived from the anion-topology by populating one half of the triangles with BO_3 triangles, each square with an MgO_6 octahedron, and each pentagon with a $Ur\phi_5$ polyhedron. The resulting sheet (Fig. 7ab) contains $Ur\phi_5$ polyhedra that share two edges with BO_3 triangles and one edge with an MgO_6 octahedron. This unusual mode of polymerization requires significant bond-angle distortion in the $Ur\phi_5$ polyhedra, owing to the substantial mismatch of the edge lengths of the ideal polyhedra, as is readily apparent from inspection of Figure 7ab. The sheets in the structure of $[Mg(UO_2)(B_2O_5)]$ are connected by the sharing of anions between MgO_6 octahedra and $Ur\phi_5$ polyhedra.

The structure of $K_2[(UO_2)(MoO_4)_2]$ (Fig. 7ae) contains an $X^{6+}O_4$ tetrahedron that shares corners with only two other polyhedra within the sheet; thus these tetrahedra become edges in the corresponding anion-topology (Fig. 7ad). Note that, in addition to triangles, squares and pentagons, this anion-topology also contains an eight-sided polygon. The anion-topology of the sheet in the structure of $K_2[(UO_2)(MoO_4)_2]$ (Fig. 7ad) contains chains of alternating edge-sharing squares and pentagons. Chains are separated by chains of edge-sharing triangles and squares, with twice as many squares as triangles. The sheet is derived by populating each pentagon with a $Ur\phi_5$ polyhedron, each triangle with a $Mo^{6+}O_4$ tetrahedron, and inserting additional $Mo^{6+}O_4$ tetrahedra such that a tetrahedron edge connects adjacent $Ur\phi_5$ polyhedra (Fig. 7ae). The sheets are connected through the interlayer K cations.

Anion-Topologies with Triangles, Squares, Pentagons and Hexagons

There are sixteen structures that are based on sheets that have triangles, squares, pentagons and hexagons in their anion-topology (Table 4). There are only five distinct anion-topologies that contain all of these polygons, and structures are grouped according to sheet anion-topology in Table 4. Notably, each of four of these anion-topologies only occurs in one structure.

Phosphuranylite anion-topology: The structure of phosphuranylite contains sheets with the anion-topology shown in Figure 8a. The anion-topology contains a chain of edge-sharing pentagons and hexagons, arranged so that dimers of edge-sharing pentagons share edges with hexagons, and there are twice as many pentagons as hexagons. Adjacent chains are offset, such that hexagons in a given chain are adjacent to pentagons in the chains on either side, and the chains of pentagons and hexagons are separated by a chain of edge-sharing squares and triangles. Five distinct populations of this anion-topology occur in twelve structures. No sheets with this anion-topology have the square sites occupied.

Several structures contain sheets in which each pentagon of the phosphuranylite anion-topology is populated by a $Ur\phi_5$ polyhedron, each hexagon by a $Ur\phi_6$ polyhedron, and the triangles are the faces of tetrahedra (Figs. 8b, c, d). In these sheets, each tetrahedron shares an edge with a $Ur\phi_6$ polyhedron and a corner with a $Ur\phi_5$ polyhedron in an adjacent chain of pentagons and hexagons (Figs. 8b, c, d). Each of these sheets has the composition $(UO_2)_3(XO_4)_2\phi_2$, where X is a tetrahedrally coordinated cation. The sheets shown in Figures 8b, 8c and 8d differ only in the orientations of the tetrahedra. In sheet 8b, along any chain of edge-sharing triangles and squares in the anion-topology, the apices of the tetrahedra point up (U) and down (D) with the sequence UUDDUU, and the tetrahedra that share an edge with a given $Ur\phi_6$ polyhedron have apices that either both point up or both point down (Fig. 8b). The resulting sheet, with all tetrahedra occupied by P, occurs in the structures of phosphuranylite, upalite, françoisite-(Nd) and dewindtite (Table 4). Of these, the structure of phosphuranylite is remarkable because it contains $Ur\phi_4$, $Ur\phi_5$ and $Ur\phi_6$ polyhedra (only the structures of phosphuranylite and vanmeersscheite contain all three types of $Ur\phi_n$ polyhedra). Only the $Ur\phi_5$ and $Ur\phi_6$

TABLE 4. STRUCTURES CONTAINING SHEETS BASED UPON ANION TOPOLOGIES CONTAINING TRIANGLES, SQUARES, PENTAGONS AND HEXAGONS

Name	Fig.	Formula	S. G.	*a* (Å)	*b* (Å)	*c* (Å)	α (°)	β (°)	γ (°)	Ref.
phosphuranylite	8b	$KCa(H_3O)_3(UO_2)[(UO_2)_3(PO_4)_2O_2]_2(H_2O)_8$	*Cmcm*	15.899	13.740	17.300				1
upalite	8b	$Al[(UO_2)_3(PO_4)_2O(OH)](H_2O)_7$	$P2_1/a$	13.704	16.82	9.332		111.5		2
françoisite-(Nd)	8b	$Nd[(UO_2)_3(PO_4)_2O(OH)](H_2O)_6$	$P2_1/c$	9.298	15.605	13.668		112.77		3
dewindtite	8b	$Pb_3[H(UO_2)_3O_2(PO_4)_2]_2(H_2O)_{12}$	*Bmmb*	16.031	17.264	13.605				4
vanmeersscheite	8c	$U(OH)_4[(UO_2)_3(PO_4)_2(OH)_2](H_2O)_4$	$P2_1mn$	17.06	16.76	7.023				5
dumontite	8c	$Pb_2[(UO_2)_3(PO_4)_2O_2](H_2O)_5$	$P2_1/m$	8.118	16.819	6.983		109.03		6
phurcalite	8d	$Ca_2[(UO_2)_3(PO_4)_2(OH)_2](OH)_2(H_2O)_4$	*Pbca*	17.415	16.035	13.598				7
phuralumite	8d	$Al_2((UO_2)_3(PO_4)_2(OH)_2)(OH)_4(H_2O)_{10}$	$P2_1/a$	13.836	20.918	9.428		112.44		8
althupite	8d	$AlTh(UO_2)[(UO_2)_3(PO_4)_2O(OH)]_2$ $(OH)_3(H_2O)_{15}$	$P\bar{1}$	10.953	18.567	13.504	72.64	68.20	84.21	9
guilleminite	8e	$Ba[(UO_2)_3(SeO_3)_2O_2](H_2O)_3$	$P2_1nm$	7.084	7.293	16.881				10
johannite	8f	$Cu[(UO_2)_2(SO_4)_2(OH)_2](H_2O)_8$	$P\bar{1}$	8.903	9.499	6.812	109.87	112.01	100.40	11
	8f	$Sr[(UO_2)_2(CrO_4)_2(OH)_2](H_2O)_8$	$P\bar{1}$	8.923	9.965	11.602	106.63	99.09	97.26	12
roubaultite	9a	$[Cu_2(UO_2)_3(CO_3)_2O_2(OH)_2](H_2O)_4$	$P\bar{1}$	7.767	6.924	7.850	92.16	90.89	93.48	13
	9d	$(UO_2)H(PO_3)_3$	$P2_1/b$	9.811	20.814	8.6947			94.09	14
	9e	$[Ca(UO_2)_2(BO_3)_2]$	*C*2	16.512	8.169	6.582		96.97		15
	9h	$(NH_4)[(UO_2)F(SeO_4)](H_2O)$	*Pnma*	8.450	13.483	13.569				16

References: (1) Demartin *et al.* (1991), (2) Piret & Declercq (1983), (3) Piret *et al.* (1988), (4) Piret *et al.* (1990), (5) Piret & Deliens (1982), (6) Piret & Piret-Meunier (1988), (7) Atencio *et al.* (1991), (8) Piret *et al.* (1979), (9) Piret & Deliens (1987), (10) Cooper & Hawthorne (1995), (11) Mereiter (1982c), (12) Serezhkin *et al.* (1982), (13) Ginderow & Cesbron (1985), (14) Sarin *et al.* (1983), (15) Gasperin (1987d), (16) Blatov *et al.* (1989).

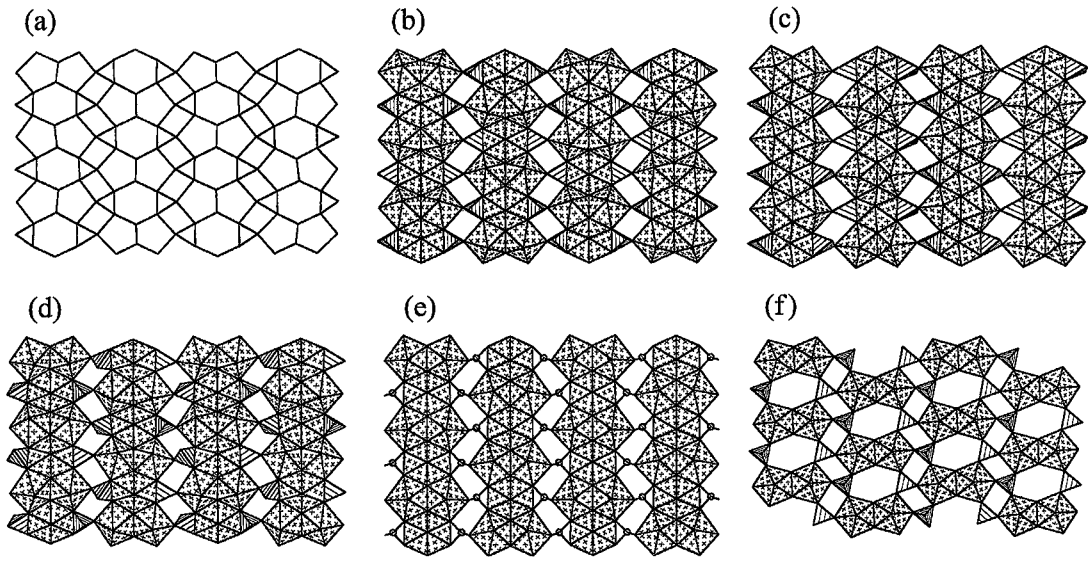

FIG. 8. Sheets based upon the phosphuranylite anion-topology. The corresponding structures are listed in Table 4. Legend as in Figure 3. In 8e, the circles represent Se^{4+} cations.

polyhedra occur within the sheets; the $Ur\phi_4$ polyhedra are located between the sheets, directly above and below the squares in the corresponding anion-topology. The uranyl ion that occurs between the sheets is parallel to the sheet, and the equatorial anions of the $Ur\phi_4$ polyhedron are also the apical anions of the PO_4 tetrahedra of sheets above and below. Additional bonding between the sheets occurs through the interlayer K and Ca cations and hydrogen bonds. In the structures of upalite, françoisite-(Nd) and dewindtite, the sheets are linked through interlayer cations and by hydrogen bonds.

Consider the sheet shown in Figure 8c: going along the chain of edge-sharing triangles and squares in the anion-topology, the apices of tetrahedra occur in the sequence UDUDUD, and the apices of both tetrahedra that share an edge with a $Ur\phi_6$ polyhedron point either up or down. This sheet is the basis of the structures of vanmeersscheite and dumontite (Table 4), where the tetrahedra contain P in both cases. The structure of vanmeersscheite contains $Ur\phi_4$, $Ur\phi_5$ and $Ur\phi_6$ polyhedra. There are two symmetrically distinct $Ur\phi_4$ polyhedra that occur between the sheets, and each provides intersheet bonding by sharing an anion with a single PO_4 tetrahedron of each sheet. Additional intersheet-linkage is provided by hydrogen bonds. The sheets in the structure of dumontite are linked through the interstitial Pb cations and through hydrogen bonds.

In the sheet shown in Figure 8d, along the chain of edge-sharing triangles and squares in the anion-topology, the apices of tetrahedra are oriented in the sequence UUDDUU. However, in contrast to sheet 8b, the apices of the two tetrahedra that share an edge with a $Ur\phi_6$ polyhedron point in opposite directions (Fig. 8d). This sheet occurs in the structures of phurcalite, phuralumite, and althupite. In the structures of phurcalite and phuralumite, the sheets are linked through interlayer cations and hydrogen bonds only. In the structure of althupite, however, there is an additional $Ur\phi_5$ polyhedron located between the sheets. Two equatorial anions of the $Ur\phi_5$ polyhedron are also apical anions of PO_4 tetrahedra of the closest sheet, and the $Ur\phi_5$ polyhedron is only linked to the other sheet by hydrogen bonding. Additional intersheet linkages are provided by intersheet cations and hydrogen bonds.

The structure of guilleminite contains the sheet shown in Figure 8e. This sheet, which is unique to guilleminite, is generated from the anion-topology shown in Figure 8a by populating each pentagon and hexagon with $Ur\phi_5$ and $Ur\phi_6$ polyhedra, respectively, and the triangles with $Se^{4+}O_3$ triangles. Owing to the lone pair of electrons on the Se cation, each anion is on the same side of the cation, forming a triangle that shares an edge with the $Ur\phi_6$ polyhedron. Bonding between the sheets occurs *via* the Ba intersheet cations and hydrogen bonds.

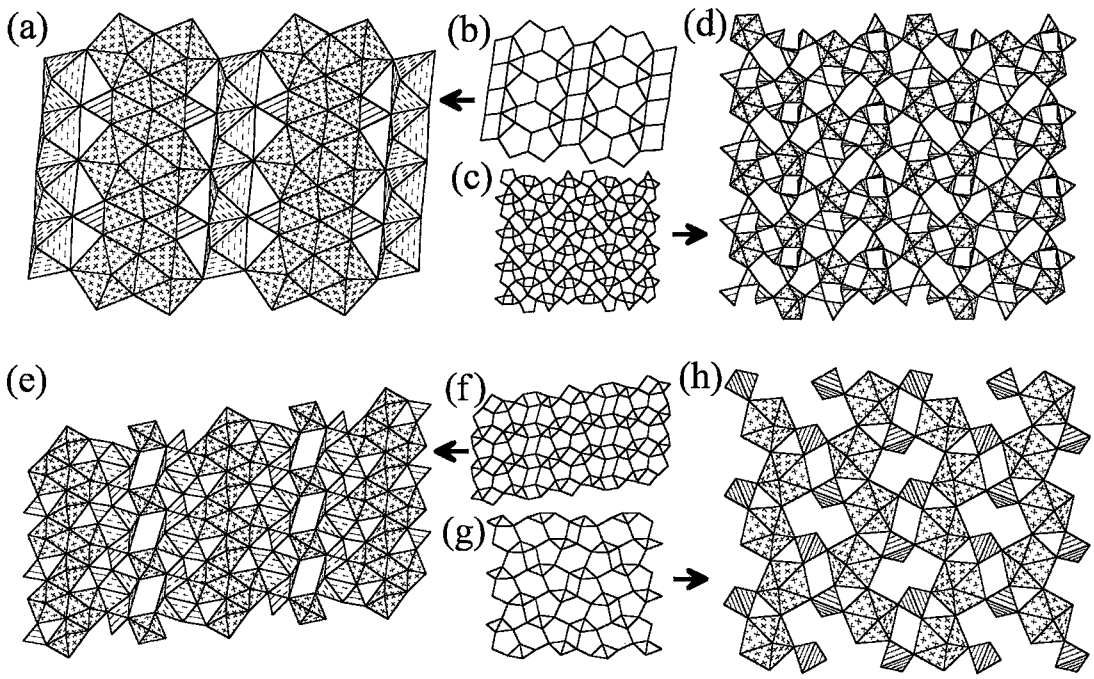

FIG. 9. Sheets based upon anion-topologies that contain triangles, squares, pentagons and hexagons. The corresponding structures are listed in Table 4. Legend as in Figure 6, except that non-U^{6+} pentagonal bipyramids are shaded with broken parallel lines.

The structures of johannite and $Sr[(UO_2)_2(CrO_4)_2(OH)_2](H_2O)_8$ (Table 4) are both based on the sheet shown in Figure 8f. This sheet is obtained from the anion-topology in Figure 8a by populating each pentagon with a $Ur\phi_5$ polyhedron, and each triangle is utilized as the face of a tetrahedron. This sheet has composition $(UO_2)_2(XO_4)_2(OH)_2$, $X = S^{6+}$ in johannite and $X = Cr^{6+}$ in $Sr[(UO_2)_2(CrO_4)_2(OH)_2](H_2O)_8$. Presumably it is not energetically favorable for an $X^{6+}O_4$ tetrahedron to share an edge with a $Ur\phi_6$ polyhedron, thus the hexagon in the anion-topology remains empty. Bonding between sheets is through intersheet cations and hydrogen bonds in both structures.

Roubaultite anion-topology: The structure of roubaultite contains the sheet shown in Figure 9a, which has the anion-topology shown in Figure 9b. The anion-topology contains the same chains of pentagons and hexagons that occur in the phosphuranylite anion-topology (Fig. 8a), but the topologies differ in the manner in which these chains are aligned and attached. In the roubaultite anion-topology, the chains are separated by an edge-sharing chain of squares that connects to the pentagons of the chain of pentagons and hexagons by sharing corners. This configuration creates groups of three edge-sharing triangles. The sheet in the structure of roubaultite is obtained by filling each pentagon with a $Ur\phi_5$ polyhedron, each hexagon with a $Ur\phi_6$ polyhedron, each square with a $Cu\phi_6$ octahedron, and the triangles that share an edge with the $Ur\phi_6$ polyhedra contain CO_3 triangles. This gives a sheet with the composition $Cu_2(UO_2)_3(CO_3)_2O_2(OH)_2$; linkages between these sheets occur through hydrogen bonds to interlayer H_2O groups only.

$(UO_2)H(PO_3)_3$ anion-topology: The structure of $(UO_2)H(PO_3)_3$ is based upon the sheet shown in Figure 9d, which has the anion-topology shown in Figure 9c. The pentagons in the anion-topology are populated by $Ur\phi_5$ polyhedra, and the triangles are the faces of PO_4 tetrahedra; the remaining polygons of the anion-topology remain empty. The sheets are linked by sharing apical anions of PO_4 tetrahedra and *via* hydrogen bonds.

$[Ca(UO_2)_2(BO_3)_2]$ anion-topology: The structure of $[Ca(UO_2)_2(BO_3)_2]$ contains sheets (Fig. 9e) with the anion-topology shown in Figure 9f. The sheet contains both $Ur\phi_4$ and $Ur\phi_5$ polyhedra, as well as CaO_7 pentagonal bipyramids and BO_3 triangles (Fig. 9e). The BO_3 triangles share edges with the CaO_7 pentagonal bipyramids, which also share edges with $Ur\phi_5$ polyhedra, and corners with $Ur\phi_4$ polyhedra (Fig. 9e). One half of the $Ur\phi_4$ polyhedra are located in chains of $Ur\phi_4$

TABLE 5. MISCELLANEOUS STRUCTURES CONTAINING SHEETS BASED UPON ANION TOPOLOGIES CONTAINING HEXAGONS

Name	Fig.	Formula	S. G.	*a* (Å)	*b* (Å)	*c* (Å)	α (°)	β (°)	γ (°)	Ref.
	10a	α-UO_3	*C2mm*	3.961	6.860	4.166				1
	10a	α-$[(UO_2)(OH)_2]$	*Cmca*	4.242	10.302	6.868				2
	10a	$Bi_2[(UO_2)O_2]O_2$	*C2*	6.872	4.009	9.690		90.16		3
	10a	$Cs_2(U_2O_7)(D_2O)_{0.444}$	*C2/m*	14.5314	4.2739	7.6011		113.02		4
	10a	$Ca[(UO_2)O_2]$	*R*$\bar{3}$*m*	6.2683			36.040			5
	10a	α-$Sr[(UO_2)O_2]$	*R*$\bar{3}$*m*	6.587			35.30			6
	10a	γ-$Sr[(UO_2)O_2]$	*R*$\bar{3}$*m*	6.542			35.54			6
	10a	α-$Cd[(UO_2)O_2]$	*R*$\bar{3}$*m*	6.233			36.12			7
	10a	$(Na_2U_2O_7)_{0.5}$	*R*$\bar{3}$*m*	6.34			36.11			8
	10a	$K_2U_2O_7$	*R*$\bar{3}$*m*	6.99			32.90			9
umohoite	10c	$[(UO_2)(MoO_4)](H_2O)_4$	$P2_1/c$	6.32	7.50	57.8		94.		10
rutherfordine	10d	$[(UO_2)(CO_3)]$	*Pmmn*	4.845	9.205	4.296				11
	10d	$[(UO_2)(SeO_3)]$	$P2_1/m$	5.408	9.278	4.2545		93.45		12
	10g	$[(UO_2)(BO_3)O]$	*C2/c*	12.504	4.183	10.453		122.18		13
	10h	$[(UO_2)TiNb_2O_8]$	*Fddd*	7.28	12.62	16.02				14
	10h	$[(UO_2)\ Nb_3O_8]$	*Fddd*	7.38	12.78	15.96				15

References: (1) Loopstra & Cordfunke (1966), (2) Taylor (1971), (3) Koster *et al.* (1975), (4) Mijlhoff *et al.* (1993), (5) Loopstra & Rietveld (1969), (6) Fujino *et al.* (1977), (7) Yamashita *et al.* (1981), (8) Kovba *et al.* (1958), (9) Jove *et al.* (1988), (10) Makarov & Anikina (1963), (11) Christ *et al.* (1955), (12) Loopstra & Brandenburg (1978), (13) Gasperin (1987e), (14) Chevalier & Gasperin (1969), (15) Chevalier & Gasperin (1968).

and $Ur\phi_5$ polyhedra that share edges, whereas the other $Ur\phi_4$ polyhedra only share corners with CaO_7 pentagonal bipyramids. The sheets are connected in the structure by sharing anions.

$(NH_4)[(UO_2)F(SeO_4)](H_2O)$ anion-topology: The structure of $(NH_4)[(UO_2)F(SeO_4)](H_2O)$ contains the sheet shown in Figure 9h, which has the anion-topology shown in Figure 9g. This unique anion-topology contains chains of corner-sharing pentagons separated by triangles, squares and hexagons. The sheet is obtained by populating each pentagon with a $Ur(\phi,F)_5$ polyhedron and one half of the triangles with $Se^{4+}O_4$ tetrahedra. The sheets are linked through hydrogen bonds to intersheet NH_4 and H_2O groups.

Other anion-topologies containing hexagons

In addition to those structures listed in Table 4, sixteen structures are based upon sheets with hexagons in their corresponding anion-topologies (Table 5). The sheets that occur in these structures have one of four underlying anion-topologies, and structures are grouped accordingly in Table 5.

α-UO_3 anion-topology: The anion-topology of the sheet that occurs in the structure of α-UO_3 contains only hexagons (Fig. 10b). Populating each hexagon with a $Ur\phi_6$ polyhedron gives the sheet shown in Figure 10a, which occurs in ten structures (Table 5). This sheet has the composition $(UO_2)\phi_2$. In the structure of α-UO_3, adjacent sheets are linked by sharing anions; in α-$(UO_2)(OH)_2$, the sheets are connected though hydrogen bonds only, and in the remaining structures, intersheet linkages occur through intersheet cations.

The structure of umohoite is based upon a sheet with the α-UO_3 anion-topology, but in this sheet only half of the hexagons are populated with $Ur\phi_6$ polyhedra; the other half are populated by $Mo^{6+}O_8$ hexagonal bipyramids (Fig. 10c). The sheets are linked through hydrogen bonds to intersheet H_2O groups.

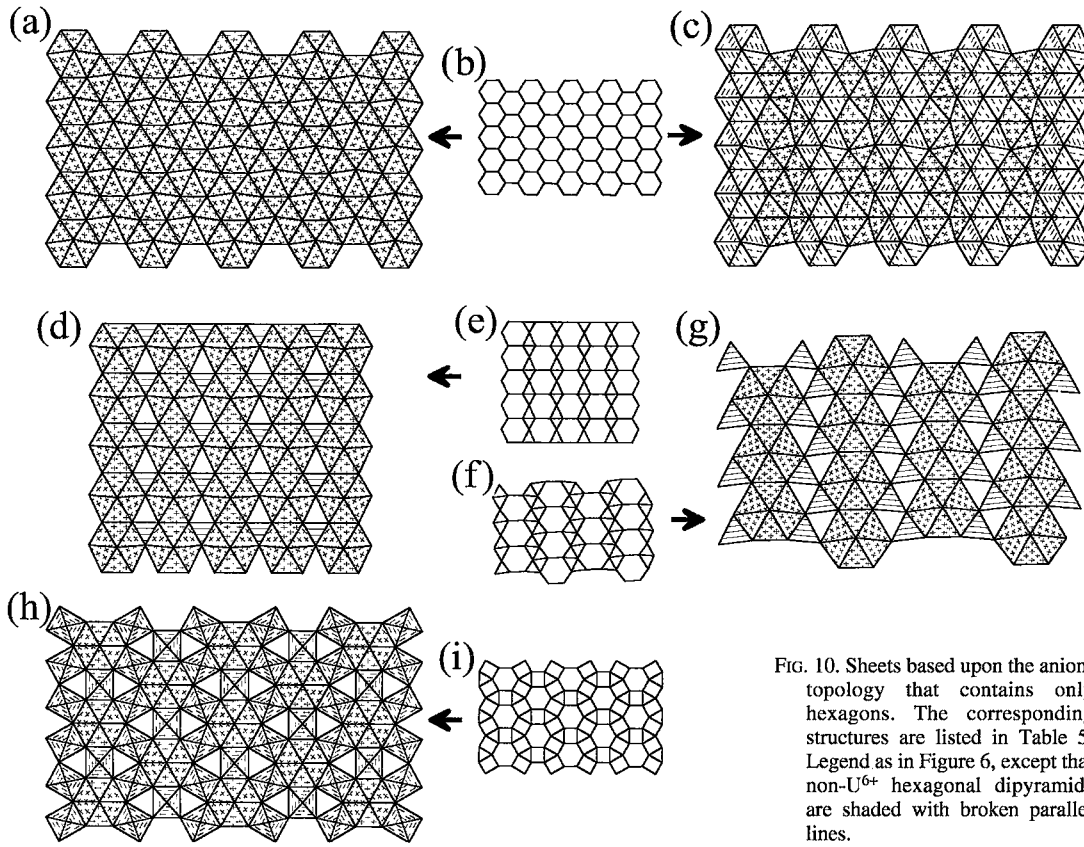

FIG. 10. Sheets based upon the anion-topology that contains only hexagons. The corresponding structures are listed in Table 5. Legend as in Figure 6, except that non-U^{6+} hexagonal dipyramids are shaded with broken parallel lines.

Rutherfordine anion-topology: The structures of rutherfordine and $[(UO_2)(SeO_3)]$ both contain sheets with the anion-topology shown in Figure 10e. This anion-topology contains parallel chains of edge-sharing hexagons that share corners, generating dimers of edge-sharing triangles (Fig. 10e). The structures of rutherfordine and $[(UO_2)(SeO_3)]$ contain the sheet shown in Figure 10d. This is obtained by populating all hexagons of the anion-topology with $Ur\phi_6$ polyhedra, and half of the triangles with CO_3 (rutherfordine) and $Se^{4+}O_3$ triangles. Sheets are linked through van der Waals bonds only.

$[(UO_2)(BO_3)O]$ anion-topology: The structure of $[(UO_2)(BO_3)O]$ contains a sheet (Fig. 10g) with the anion-topology shown in Figure 10f. This anion-topology contains parallel chains of edge-sharing hexagons that are connected by sharing edges with a chain of edge-sharing triangles (Fig. 10f). The sheet shown in Figure 10g is obtained by populating each hexagon in the anion-topology with a $Ur\phi_6$ polyhedron, and every second triangle of the edge-sharing chains of triangles with a BO_3 triangle. The sheets are linked through van der Waals forces only.

$[(UO_2)Nb_3O_8]$ anion-topology: The structures of $[(UO_2)Nb_3O_8]$ and $[(UO_2)TiNb_2O_8]$ are based upon sheets with the anion-topology shown in Figure 10i. This anion-topology contains parallel chains of alternating edge-sharing squares and hexagons separated by chains of alternating edge-sharing triangles and squares. The arrangement is such that each edge of a hexagon is shared with a square, and each corner is shared with a triangle. The structure of $[(UO_2)Nb_3O_8]$ is based on the sheet shown in Figure 10h. This sheet is obtained from the anion-topology by populating each hexagon with a $Ur\phi_6$ polyhedron, two-thirds of the squares with $Nb^{5+}O_6$ octahedra, the remaining squares with $Nb^{4+}O_6$ octahedra, and the triangles remain empty. The sheet in the structure of $[(UO_2)TiNb_2O_8]$ is similar, differing only in that one-third of the square sites of the anion-topology are populated by $Ti^{4+}O_6$ octahedra. The sheets are linked by sharing anions in both of these structures. The O_{Ur} atoms are also apical oxygen atoms in the $(Nb,Ti)O_6$ octahedra in adjacent sheets, and corner-sharing between $(Nb,Ti)O_6$ octahedra of adjacent sheets also occurs.

Infinite Chains

Currently, nineteen structures are known that are based upon infinite chains of cation polyhedra of higher bond-valence (Table 6). Eight distinct chain-

TABLE 6. STRUCTURES BASED UPON INFINITE CHAINS

Name	Fig.	Formula	S. G.	*a* (Å)	*b* (Å)	*c* (Å)	α (°)	β (°)	γ (°)	Ref.
	11a	$Na_4[(UO_2)O_3]$	*I4/m*	7.5571		4.6411				1
	11a	$Ca_2[(UO_2)O_3]$	$P2_1/c$	7.9137	5.4409	11.4482		108.803		2
	11a	$Sr_2[(UO_2)O_3]$	$P2_1/c$	8.1043	5.6614	11.9185		108.985		2
	11a	$Li_4[(UO_2)O_3]$	*I4/m*	6.725		4.451				3
moctezumite	11b	$PbTe[(UO_2)O_3]$	$P2_1/c$	7.813	7.061	13.775		93.71		4
	11b	$[(UO_2)Cl_2H_2O]$	$P2_1/m$	5.828	8.534	5.557		97.79		5
derriksite	11c	$Cu_4[(UO_2)(SeO_3)_2](OH)_6$	$Pn2_1m$	5.570	19.088	5.965				6
	11d	$[(UO_2)(HSeO_3)_2(H_2O)]$	*A2/a*	6.354	12.578	9.972		82.35		7
demesmaekerite	11e	$Pb_2Cu_5[(UO_2)(SeO_3)_3]_2(OH)_6(H_2O)_2$	$P\bar{1}$	11.955	10.039	5.639	89.78	100.36	91.34	8
walpurgite	11f	$Bi_4O_4[(UO_2)(AsO_4)_2](H_2O)_2$	$P\bar{1}$	7.135	10.426	5.494	101.47	110.82	88.20	9
orthowalpurgite	11f	$Bi_4O_4[(UO_2)(AsO_4)_2](H_2O)_2$	*Pbcm*	5.492	13.324	20.685				10
	11f	$Cu_4[(UO_2)(MoO_4)_2](OH)_6$	*B2/m*	19.8392	5.5108	6.1009			104.477	11
	11g	$[(UO_2)(H_2PO_4)_2(H_2O)](H_2O)_2$	$P2_1/c$	11.369	13.899	7.481		113.67		12
	11g	$Mn[(UO_2)(SO_4)_2(H_2O)](H_2O)_4$	$P2_1$	6.506	11.368	8.338		90.79		13
	11h	$[(UO_2)(CrO_4)(H_2O)_2](H_2O)_{3.5}$	$P2_1/c$	11.179	7.119	26.49		94.19		14
	11h	$[(UO_2)(SO_4)(H_2O)_2](H_2O)_{1.5}$	*C2/c*	13.70	10.79	11.91		110.8		15
	11h	$[(UO_2)(SO_4)(H_2O)_2](H_2O)_{0.5}$	$P2_1/a$	16.887	12.492	6.7354		90.88		16
	11h	$[(UO_2)(SO_4)(H_2O)_2]_2(H_2O)_3$	$P2_1ca$	11.227	6.790	21.186				17
	11h	$[(UO_2)(SeO_4)(H_2O)_2](H_2O)_2$	*C2/c*	14.653	10.799	12.664		119.95		18

References: (1) Wolf & Hoppe (1986), (2) Loopstra & Rietveld (1969), (3) Reshetov & Kovba (1966), (4) Swihart *et al.* (1993), (5) Taylor & Wilson (1974), (6) Ginderow & Cesbron (1983a), (7) Mistryukov & Michailov (1983), (8) Ginderow & Cesbron (1983b), (9) Mereiter (1982b), (10) Krause *et al.* (1995), (11) Tali *et al.* (1993), (12) Krogh-Andersen *et al.* (1985), (13) Tabachenko *et al.* (1979), (14) Serezhkin & Trunov (1981), (15) Brandenburg & Loopstra (1973), (16) van der Putten & Loopstra (1974), (17) Zalkin *et al.* (1978), (18) Serezhkin *et al.* (1981a).

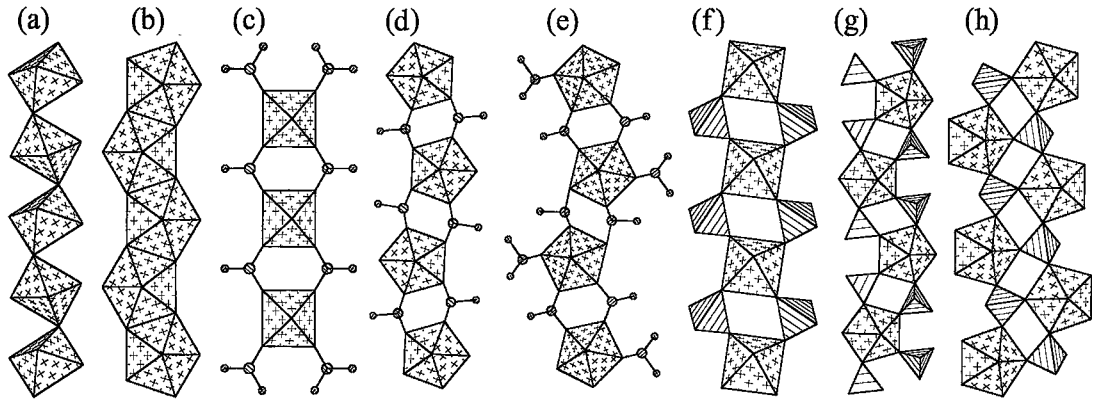

FIG. 11. Chains of polyhedra that occur in the structures of uranyl phases. The corresponding structures are listed in Table 6. Legend as in Figure 3. Circles shaded with parallel lines represent Se^{4+} cations.

topologies occur (Fig. 11), and the structures are grouped according to chain topology in Table 6. In these structures, the chains are bonded together through interstitial cation polyhedra of lower bond-valence and through hydrogen bonds.

Two of the chain topologies contain only uranyl polyhedra (Figs. 11a, b). The chain illustrated in Figure 11a is formed by the sharing of a single anion between $Ur\phi_4$ polyhedra, giving a chain with composition $(UO_2)O_3$. This anhydrous chain occurs in the structures of $Na_4[(UO_2)O_3]$, $Ca_2[(UO_2)O_3]$, $Sr_2[(UO_2)O_3]$ and $Li_4[(UO_2)O_3]$. Note that this chain also is a component of the sheet shown in Figure 4b, which occurs in seven structures. The structures of moctezumite and $[(UO_2)Cl_2H_2O]$ are both based upon chains of edge-sharing $Ur(\phi,Cl)_5$ polyhedra (Fig. 11b) with composition $(UO_2)(\phi,Cl)_3$. This chain of edge-sharing $Ur\phi_5$ polyhedra occurs repeatedly in various sheets (Figs. 5a, 5d, 6, 7d, 7h).

The chain topologies illustrated in Figures 11c, 11d and 11e are restricted to selenium-bearing phases. The structure of derriksite is the only one known to contain the chain shown in Figure 11c. The chain contains $Ur\phi_4$ polyhedra, each of which shares corners with four $Se^{4+}\phi_3$ triangles, giving a chain of composition $(UO_2)(SeO_3)_2$. The structure of $[(UO_2)(HSeO_3)_2(H_2O)]$ is based on the chain shown in Figure 11d. The chain contains $Ur\phi_5$ polyhedra, each of which shares corners with four $Se^{4+}\phi_3$ triangles, giving a chain with composition $(UO_2)(SeO_3)_2\phi$. The structure of demesmaekerite contains the chain shown in Figure 11e, which is derived from the chain in Figure 11d by attaching additional $Se^{4+}\phi_3$ triangles to the $Ur\phi_5$ polyhedra, giving a chain with the composition $(UO_2)(SeO_3)_2$.

The structures of walpurgite, orthowalpurgite and $Cu_4[(UO_2)(MoO_4)_2](OH)_6$ are based upon the chain illustrated in Figure 11f. The chain is constructed from $Ur\phi_4$ polyhedra and $X\phi_4$ tetrahedra, where $X = As^{5+}$ in walpurgite and orthowalpurgite, and $X = Mo^{6+}$ in $Cu_4[(UO_2)(MoO_4)_2](OH)_6$. Each $Ur\phi_4$ polyhedron shares corners with four XO_4 tetrahedra, giving a chain with the composition $(UO_2)(XO_4)_2$. This chain is also a component of the sheet shown in Figure 4c, which occurs in fifteen structures.

Two chain topologies are based upon corner-sharing of XO_4 tetrahedra and $Ur\phi_5$ polyhedra (Figs. 11g, h). The chain illustrated in Figure 11g has a composition $(UO_2)(XO_4)_2\phi$. This chain is the basis of the structures of $[(UO_2)(H_2PO_4)_2(H_2O)](H_2O)_2$, where $X = P$, and $Mn[(UO_2)(SO_4)_2(H_2O)](H_2O)_4$, in which $X = S^{6+}$. In this chain, each $Ur\phi_5$ polyhedron shares corners with four XO_4 tetrahedra. The chain illustrated in Figure 11h is the basis of five structures (Table 6) and, in this case, each $Ur\phi_5$ polyhedron shares a corner with only three XO_4 tetrahedra. This results in a chain with composition $(UO_2)(XO_4)\phi_2$, with X being Cr^{6+}, S^{6+} and Se^{6+}. Note that this chain also occurs as part of the sheet shown in Figure 8c.

FINITE CLUSTERS

Twenty-two structures are based upon isolated clusters of cation polyhedra of higher bond-valence (Table 7). The clusters of polyhedra are linked through interstitial low-valence cation-polyhedra such as $Ca\phi_n$, $K\phi_n$, $Na\phi_n$, *etc.*, and through hydrogen bonds. There are only ten topologically distinct clusters (Fig. 12), and the structures are grouped according to the topology of the polyhedral cluster in Table 7.

The most common finite cluster has the composition $(UO_2)(XO_3)_3$ (X = C, N), and is composed of a $Ur\phi_6$ polyhedron that shares three equatorial edges with XO_3 triangles (Fig. 12a). All but one of the occurrences of this finite cluster contain carbonate triangles, whereas one contains nitrate triangles. The

TABLE 7. STRUCTURES BASED UPON FINITE CLUSTERS

Name	Fig.	Formula	S. G.	a (Å)	b (Å)	c (Å)	α (°)	β (°)	γ (°)	Ref.
liebigite	12a	$Ca_2[(UO_2)(CO_3)_3](H_2O)_{11}$	*Bba2*	16.699	17.557	13.697				1
schröckingerite	12a	$NaCa_3[(UO)_2(CO_3)_3](SO_4)F(H_2O)_{10}$	$P\bar{1}$	9.634	9.635	14.391	91.41	92.33	120.26	2
bayleyite	12a	$Mg_2[(UO_2)(CO_3)_3](H_2O)_{18}$	$P2_1/a$	26.560	15.256	6.505		92.90		3
swartzite	12a	$CaMg[(UO_2)(CO_3)_3](H_2O)_{12}$	$P2_1/m$	11.080	14.634	6.439		99.43		4
andersonite	12a	$Na_2Ca[(UO_2)(CO_3)_3](H_2O)_5$	$R\bar{3}m$	17.904		23.753				5
	12a	$Cs_4[(UO_2)(CO_3)_3](H_2O)_6$	$P2_1/n$	18.723	9.647	11.297		96.84		6
	12a	$Sr_2[(UO_2)(CO_3)_3](H_2O)_8$	$P2_1/c$	11.379	11.446	25.653		93.40		7
	12a	$(NH_4)_4[(UO_2)(CO_3)_3]$	$C2/c$	10.679	9.373	12.850		96.43		8
	12a	$Rb[(UO_2)(NO_3)_3]$	$R\bar{3}c$	9.384		18.899				9
	12b	$Rb_2[(UO_2)(NO_3)_4]$	$P2_1/c$	6.42	7.82	12.79		108.68		10
	12c	$[(UO_2)(NO_3)_2](H_2O)_6$	$Cmc2_1$	13.197	8.035	11.467				11
	12c	$[(UO_2)(NO_3)_2](H_2O)_2$	$P2_1/c$	14.124	8.432	7.028		108.0		12
	12d	$[(UO_2)_2(OH)_2(NO_3)_2](H_2O)_4$	$P\bar{1}$	8.622	8.628	10.393	109.57	105.56	99.65	13
	12e	$K_4[(UO_2)(SO_4)_3]$	*Pnma*	13.053	23.200	9.379				14
	12f	$[(UO_2)_4Cl_2O_2(OH)_2(H_2O)_6](H_2O)_4$	$P2_1/n$	11.645	10.101	10.206		105.77		15
	12f	$Rb_4[(UO_2)_4O_2Cl_8(H_2O)_2](H_2O)_2$	$P2_1/c$	8.540	8.096	21.735		111.74		16
	12f	$K_2[(UO_2)_4Cl_4O_2(OH)_2(H_2O)_4]\ (H_2O)_2$	$P\bar{1}$	12.15	12.33	8.026	110.50	96.30	138.71	17
	12f	$Cs_{0.9}[(UO_2)OCl_{0.9}]$	$P2_1/m$	8.734	4.118	7.718		105.26		18
	12g	$[(UO_2)_3O(OH)_3(H_2O)_6](NO_3)(H_2O)_4$	$P\bar{1}$	8.026	11.276	12.346	109.65	99.39	88.62	19
	12h	$K_8[(UO_2)_2O_6]$	$P\bar{1}$	6.4738	9.6979	6.3438	101.17	102.30	109.02	20
	12i	$[(UO_2)(OH)Cl(H_2O)_2]$	$P2_1/n$	17.743	6.136	10.725		95.52		21
	12j	$K_6[(UO_2)B_{16}O_{24}(OH)_8](H_2O)_{12}$	$P2_1/n$	12.024	26.45	12.543		94.74		22

References: (1) Mereiter (1982a), (2) Mereiter (1986a), (3) Mayer & Mereiter (1986), (4) Mereiter (1986b), (5) Mereiter (1986c), (6) Mereiter (1988), (7) Mereiter (1986d), (8) Serezhkin *et al.* (1983), (9) Zalkin *et al.* (1989), (10) Kapshukov *et al.* (1971), (11) Taylor & Mueller (1965), (12) Dalley *et al.* (1971), (13) Perrin (1976), (14) Mikhailov *et al.* (1977), (15) Åberg (1976), (16) Perrin (1977), (17) Perrin & le Marouille (1977), (18) Allpress & Wadsley (1964), (19) Åberg (1978), (20) Wolf & Hoppe (1986), (21) Åberg (1969), (22) Behm (1985).

$(UO_2)(CO_3)_3$ cluster (Fig. 12a) occurs in carbonate-rich fluids with high pH (Langmuir 1978), and minerals growing in such solutions will commonly incorporate this cluster. Note that polymerization of this cluster is not possible because substantial over-bonding of the oxygen atoms would occur.

Notably, all finite clusters that contain carbonate triangles are the type shown in Figure 12a, whereas nitrate triangles occur in four distinct clusters (Figs. 12a, b, c, d). In the structures, $<^{[3]}C–O>$ and $<^{[3]}N–O>$ distances are approximately equal to 1.28 and 1.26 Å, respectively. If the triangles are assumed to be planar, edge lengths expected for CO_3 and NO_3 triangles are 2.22 and 2.18 Å, respectively. These edge lengths are substantially shorter than the average equatorial edge-length of the $Ur\phi_6$ polyhedron (≈ 2.47 Å), thus significant bond-angle distortion in the $Ur\phi_6$ polyhedron is required in order for edge-sharing to occur. Where the triangular polyhedron is CO_3, the cluster in which three edges of the $Ur\phi_6$ polyhedron are shared by CO_3 triangles occurs exclusively, whereas the additional $Ur\phi_6$ bond-angle distortion required for sharing edges with the somewhat smaller NO_3 triangle and, to some extent, the higher cation charge of N^{5+}, favor the sharing of only two $Ur\phi_6$ polyhedron edges with triangles, as is the case in the clusters illustrated in Figures 12b, 12c and 12d. Of these, the cluster in Figure 12c, with CO_3 triangles rather than NO_3, is a component of the sheet in the structure of roubaultite (Fig. 9a), and with $Se^{4+}O_3$ triangles it occurs in the sheet in the structure of guilleminite (Fig. 8e).

The structure of $[(UO_2)_2(OH)_2(NO_3)_2](H_2O)_4$ is based upon the cluster shown in Figure 12d. The cluster contains $Ur\phi_5$ and $Ur\phi_6$ polyhedra that share an edge, and the $Ur\phi_6$ polyhedron shares edges with two NO_3 triangles.

The structure of $K_4[(UO_2)(SO_4)_3]$ is based on a large cluster with composition $(UO_2)_2(SO_4)_6$ (Fig. 12e). This cluster contains two $Ur\phi_5$ polyhedra that do not share any anions directly, but are connected through sharing corners with two SO_4 tetrahedra. In addition, each $Ur\phi_5$ polyhedron is connected to two other SO_4 tetrahedra,

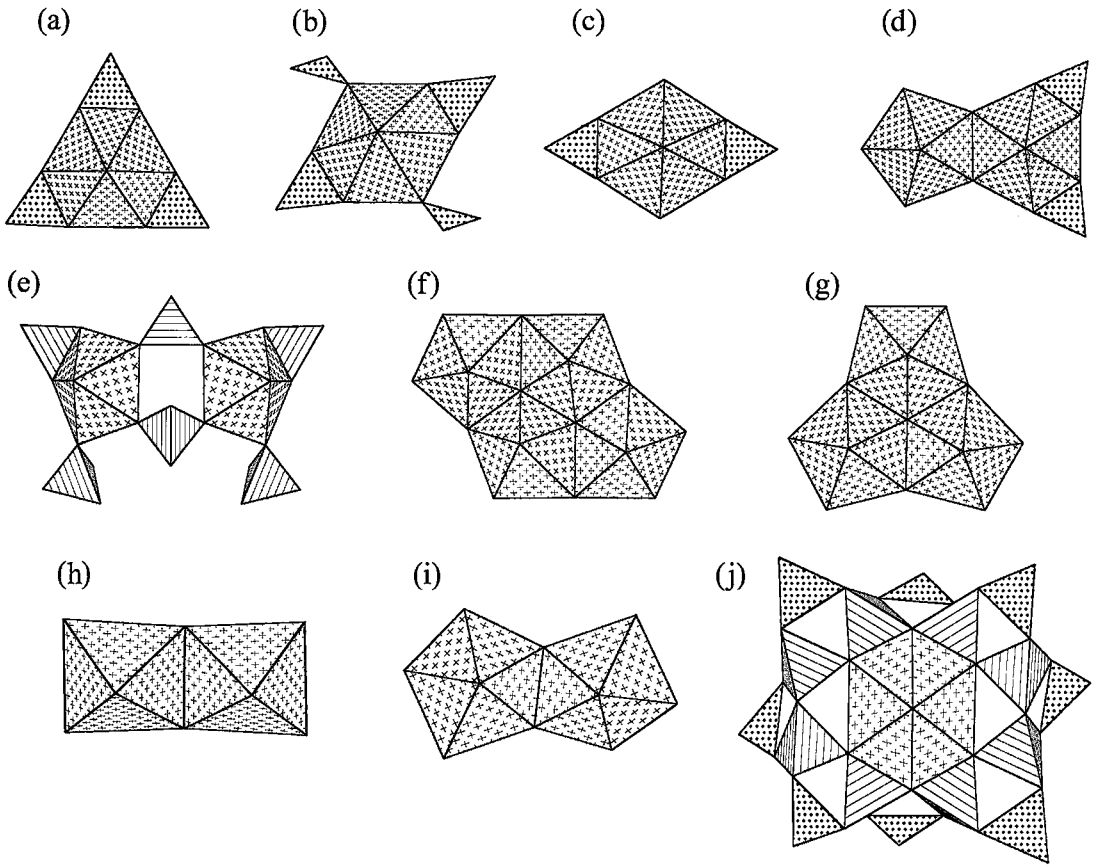

FIG. 12. Clusters of polyhedra that occur in the structures of uranyl phases. The corresponding structures are listed in Table 7. Legend as in Figure 3, except that CO_3, NO_3 and BO_3 triangles are stippled.

one by sharing corners and one by sharing edges. The $<^{[4]}S^{6+}$–O> distance in crystal structures is ~1.48 Å, giving an estimated edge-length of 2.42 Å, which is only a fair match for the ideal equatorial edge-length of the $Ur\phi_5$ polyhedron (2.75 Å). This structure is the only example found of a U^{6+} polyhedron sharing an edge with an $X^{6+}O_4$ tetrahedron; this scarcity is probably caused by the Coulombic repulsion of U^{6+} and X^{6+}.

The clusters illustrated in Figures 12f, 12g, 12h and 12i contain only uranyl polyhedra. The cluster shown in Figure 12f occurs in four structures, and the remaining three are known from only one structure each (Table 7). Because of the dominance of infinite sheet structures in uranyl phases (see above), it is remarkable that there are finite clusters of edge-sharing uranyl polyhedra. Each of the clusters is a component of a known sheet. However, each cluster (except Fig. 12h) is truncated by equatorial anions that are either Cl^-, OH^-, or H_2O. Thus, the possibilities for further polymerization are reduced relative to the case where these anions are O^{2-}. Three of these clusters contain edge-sharing $Ur(\phi,Cl)_5$ polyhedra only; these structures are consistent with the usual edge-sharing of $Ur(\phi,Cl)_5$ polyhedra in sheets. However, the structure of $K_8[(UO_2)_2O_6]$ is unusual because it contains an edge-sharing dimer of $Ur\phi_4$ polyhedra. In this configuration, the U^{6+} cations are quite close together, causing a significant Coulombic repulsion, as evidenced by the rarity of edge-sharing $Ur\phi_4$ polyhedra, which are only known to occur in two structures ($K_8[(UO_2)_2O_6]$ and $Cs_4[(UO_2)_5O_7]$).

The structure of $K_6[(UO_2)B_{16}O_{24}(OH)_8](H_2O)_{12}$ contains a large cluster with the composition $(UO_2)B_{16}O_{24}(OH)_8$ (Fig. 12j). The cluster contains a single $Ur\phi_6$ polyhedron, eight $B\phi_4$ tetrahedra, and eight $B\phi_3$ triangles. Eight three-membered rings of borate polyhedra, each with two $B\phi_4$ tetrahedra and one $B\phi_3$ triangle, form a larger ring by sharing $B\phi_4$ tetrahedra. From the descriptor for borate clusters proposed

by Burns *et al.* (1995), the cluster can be written 8Δ8□:<<Δ2□>–>. The $Ur\phi_6$ polyhedron is at the center of the larger borate ring (Fig. 12j), where it is joined to eight $B\phi_4$ tetrahedra, four by sharing edges and four by sharing corners.

Isolated Polyhedra

Seven structures contain isolated $Ur\phi_n$ polyhedra, and some details of each are given in Table 8. In each structure, isolated polyhedra of higher bond-valence are linked through low-valence cation polyhedra or by hydrogen bonds to H_2O groups. In the structures of Pb_3UO_6, Ca_3UO_6, Sr_3UO_6, $K_2Li_4UO_6$ and Li_6UO_6, the U^{6+} cation is octahedrally coordinated, and no uranyl ion is apparent. The structure of $Cs_2[(UO_2)Cl_4]$ contains a $Ur(Cl)_4$ polyhedron, with chlorine atoms located at the equatorial positions. The structure of $[(UO_2)Cl_2(H_2O)_3]$ contains a $Ur(\phi,Cl)_5$ polyhedron, with two of the equatorial anions being chlorine, and the others being H_2O groups.

Framework Structures

Twenty-six phases with structures based on frameworks of cation polyhedra of higher bond-valence are listed in Table 9. In framework structures, bond strengths in all three dimensions are similar. Many of these structures contain the $Ur\phi_4$, $Ur\phi_5$ and $Ur\phi_6$ polyhedra that are observed in most other U^{6+} phases. However, several of these structures do not contain the uranyl ion; instead, the U^{6+} cation is coordinated in some other way.

Structures that contain only $U\phi_n$ polyhedra

There are five framework structures that contain only $U\phi_n$ polyhedra, and four of these are polymorphs of UO_3 (Table 9). The structure of γ-UO_3 (Fig. 13a) contains two symmetrically distinct $Ur\phi_4$ polyhedra. The $Ur(1)\phi_4$ polyhedron shares each of its equatorial anions with $Ur(2)\phi_4$ polyhedra, but the O_{Ur} atoms are only [1]-connected. All of the anions of the $Ur(2)\phi_4$ polyhedron are shared with $Ur(1)\phi_4$ polyhedra, and the O_{Ur} atoms are equatorial anions of adjacent polyhedra. Thus, this structure contains atoms of oxygen that are bonded to one, two and three cations. The structure of β-UO_3 (Fig. 13b) contains five symmetrically distinct U^{6+} positions, but none is occupied by a uranyl ion. Two U^{6+} cations are coordinated by six oxygen atoms, whereas the remaining three are each coordinated by seven anions. The polyhedra are highly irregular, with considerable ranges of bond lengths. Polyhedra share corners and edges to form the framework. The high-pressure form of UO_3 (designated UO_3 HP) contains only one symmetrically distinct U position, and it is occupied by a nearly linear uranyl ion (O–U–O bond angle 172.3°). The uranyl ion is coordinated by five anions, but the anions are distributed such that only three are roughly within the plane that runs through the U^{6+} cation and is perpendicular to the uranyl ion; the other two occur significantly above and below the plane. The uranyl polyhedra are linked by sharing corners and edges to form the framework (Fig. 13c). The perovskite-like structure of δ-UO_3 (Fig. 13d) has cubic symmetry, and the U^{6+} cation occurs in a holosymmetric octahedron. The UO_6 octahedra link by sharing corners to form the framework.

The structure of $(UO_2)Cl_2$ (Fig. 13e) contains a single symmetrically distinct $Ur(\phi,Cl)_5$ polyhedron. Four of the equatorial anions are chlorine atoms, and the other is an oxygen atom. The polyhedra are linked by sharing edges to form chains identical to the chains in the structures of moctezumite and $(UO_2)Cl_2(H_2O)$ (Fig. 11b). The chains are linked into a framework by one of the two O_{Ur} atoms of the uranyl ion, which is an equatorial anion in a polyhedron of an adjacent chain (Fig. 13e).

TABLE 8. STRUCTURES CONTAINING ISOLATED POLYHEDRA

Name	Formula	S. G.	*a* (Å)	*b* (Å)	*c* (Å)	α (°)	β (°)	γ (°)	Ref.
	Pb_3UO_6	*Pnam*	13.719	12.351	8.213				1
	Ca_3UO_6	$P2_1/n$	5.7292	5.962	8.2991		90.56		2
	Sr_3UO_6	$P2_1/n$	6.0126	6.2138	8.6139		90.239		3
	$K_2Li_4UO_6$	$P\bar{3}m$	6.1927		5.3376				4
	Li_6UO_6	$R\bar{3}$	8.3807		7.3834				5
	$Cs_2[(UO_2)Cl_4]$	*Cm*	12.005	7.697	5.850		100.00		6
	$[(UO_2)Cl_2(H_2O)_3]$	*Pnma*	12.738	10.495	5.547				7

References: (1) Sterns *et al.* (1986), (2) van Duivenboden & Ijdo (1986), (3) Ijdo (1993b), (4) Wolf & Hoppe (1987), (5) Wolf & Hoppe (1985), (6) Tutov *et al.* (1991), (7) Debets (1968).

TABLE 9. INFINITE FRAMEWORK STRUCTURES

Name	Fig.	Formula	S. G.	*a* (Å)	*b* (Å)	*c* (Å)	α (°)	β (°)	γ (°)	Ref.
	13a	γ-UO_3	$I4_1/amd$	6.9013		19.9754				1
	13b	β-UO_3	$P2_1$	10.34	14.33	3.910		99.03		2
	13c	UO_3 HP	$P2_12_12_1$	7.511	5.466	5.224				3
	13d	δ-UO_3	$Pm\bar{3}m$	4.165						4
	13e	$(UO_2)Cl_2$	*Pnma*	5.725	8.409	8.720				5
	13f	Ba_2MgUO_6	$Fm\bar{3}m$	8.379						6
	13g	$K_9BiU_6O_{24}$	$Pm\bar{3}m$	8.631						7
	13h	$Na_2(UO_2)(SiO_4)$	$I4_1/acd$	12.718		13.376				8
	13i	β-$Cd(UO_2)O_2$	*Cmmm*	7.023	6.849	3.514				9
	—	$Cu(UO_2)O_2$	$P2_1/m$	5.475	4.957	6.569		118.87		10
	—	$Mn(UO_2)O_2$	*Imma*	6.647	6.984	6.750				11
	13j	UCr_2O_6	$P\bar{3}1m$	4.988		4.620				12
	13k	$(UO_2)(MoO_4)$	$P2_1/c$	7.202	5.484	13.599		104.54		13
	13k	α-$(UO_2)(SeO_4)$	$P2_1/c$	6.909	5.525	13.318		103.79		14
	13k	β-$(UO_2)(SO_4)$	$P2_1/c$	6.760	5.711	12.824		102.91		14
	13*l*	α-$(UO_2)(MoO_4)(H_2O)_2$	$P2_1/c$	13.612	11.005	10.854		113.05		15
	13m	$Sr(UO_2)_6(MoO_4)_7(H_2O)_{19}$	$C222_1$	11.166	20.281	24.061				16
	13n	$Ba(UO_2)_3(MoO_4)_4(H_2O)_4$	*Pbca*	17.797	11.975	23.33				17
	13o	$Mg(UO_2)_3(MoO_4)_4(H_2O)_8$	$Cmc2_1$	17.105	13.786	10.908				18
	13p	$U^{4+}(UO_2)(PO_4)_2$	$P\bar{1}$	8.8212	9.2173	5.4772	102.62	97.75	102.46	19
	13q	$Na_2(UO_2)(P_2O_7)$	$Pna2_1$	13.259	8.127	6.973				20
soddyite	13r	$(UO_2)_2(SiO_4)(H_2O)_2$	*Fddd*	8.334	11.212	18.668				21
	13r	$(UO_2)_2(GeO_4)(H_2O)_2$	*Fddd*	8.179	11.515	19.397				22
	13s	$Pb_2(UO_2)(TeO_3)_3$	$P2_1/n$	11.605	13.389	6.981		91.23		23
weeksite	13t	$(K_{0.62}Na_{0.38})_2(UO_2)_2(Si_5O_{13})(H_2O)_3$	*Cmmm*	7.092	17.888	7.113				24
cliffordite	13u	$(UO_2)(Te_3O_7)$	$Pa\bar{3}$	11.335						25

References: (1) Loopstra *et al.* (1977), (2) Debets (1966), (3) Siegel *et al.* (1966), (4) Weller *et al.* (1988), (5) Taylor & Wilson (1973), (6) Padel *et al.* (1972), (7) Gasperin *et al.* (1991), (8) Shashkin *et al.* (1974), (9) Yamashita *et al.* (1981), (10) Siegel & Hoekstra (1968), (11) Bacmann & Bertaut (1966), (12) Hoekstra & Siegel (1971), (13) Serezhkin *et al.* (1980a), (14) Brandenburg & Loopstra (1978), (15) Serezhkin *et al.* (1980b), (16) Tabachenko *et al.* (1984b), (17) Tabachenko *et al.* (1984a), (18) Tabachenko *et al.* (1983), (19) Bénard *et al.* (1994), (20) Linde *et al.* (1984), (21) Demartin *et al.* (1992), (22) Legros & Jeannin (1975), (23) Branstätter (1981a), (24) Baturin & Sidorenko (1985), (25) Branstaetter (1981b).

Structures containing $U\phi_6$ ($Ur\phi_4$) polyhedra and other cation polyhedra

The perovskite-like structures of Ba_2MgUO_6 (Fig. 13f) and $K_9BiU_6O_{24}$ (Fig. 13g) are both closely related to the structure of δ-UO_3 (Fig. 13d). Both of these structures have cubic symmetry, and the U^{6+} cation is in a holosymmetric octahedral coordination. The structure of Ba_2MgUO_6 is derived from the structure of δ-UO_3 by doubling the length of the unit-cell edge, replacing half of the UO_6 octahedra with MgO_6 octahedra, and inserting Ba cations into 12-coordinated sites in the channels that are parallel to [100] (Fig. 13f). The structure of $K_9BiU_6O_{24}$ is derived by doubling the length of the unit-cell edge, replacing one-eighth of the UO_6 octahedra with BiO_6 octahedra, one-eighth with KO_6 octahedra, and inserting K cations into the 12-coordinated sites in the channels (Fig. 13g).

The structure of $Na_2(UO_2)(SiO_4)$ (Fig. 13h) contains U^{6+} cations in pseudo-octahedral coordination, with four short (~2.0 Å) and two long (~2.3 Å) U–O bond-lengths. Four of the UO_6 octahedron anions are shared with SiO_4 tetrahedra to form a framework structure, with the Na cations located in channels parallel to [001] (Fig. 13h).

The structure of β-$Cd(UO_2)O_2$ (Fig. 13i) contains a $Ur\phi_4$ polyhedron and a CdO_6 octahedron. The uranyl ion U–O bond-length is 1.90 Å, a value considerably

longer than the average U–O bond-length in the uranyl ion in $Ur\phi_4$ polyhedra. The O_{Ur} atoms also bond to two Cd cations, and a long U–O bond-length is necessary to prevent overbonding. Adjacent $Ur\phi_4$ polyhedra share an equatorial edge, and each equatorial anion is also bonded to a Cd cation, resulting in a tighly bonded framework (Fig. 13i). The structures of $Cu(UO_2)O_2$ and $Mn(UO_2)O_2$ have the same connectivity as the β-$Cd(UO_2)O_2$ structure, although these phases are not isostructural (their symmetries are different).

The structure of $UCr^{6+}O_6$ (Fig. 13j) contains both U^{6+} and Cr^{6+} cations in holosymmetric octahedral coordination. The structure contains sheets of edge-sharing $Cr^{6+}\phi_6$ octahedra with one-third of the octahedral sites vacant. The $U^{6+}O_6$ octahedra are located between the sheets of $Cr^{6+}O_6$ octahedra, such that they share a face with a *vacant* octahedron in the sheet on either side.

Structures containing $Ur\phi_5$ polyhedra and other cation polyhedra

The compounds $(UO_2)(MoO_4)$, α-$(UO_2)(SeO_4)$ and β-$(UO_2)(SO_4)$ are isostructural (Table 9). The structure of $(UO_2)(MoO_4)$ is shown in Figure 13k. These structures contain $Ur\phi_5$ polyhedra and $X^{6+}O_4$ tetrahedra. Each $Ur\phi_5$ polyhedron shares four of its equatorial anions with $X^{6+}O_4$ tetrahedra, and the fifth equatorial anion is an O_{Ur} atom in the adjacent $Ur\phi_5$ polyhedron. The $X^{6+}O_4$ tetrahedron shares each corner with a $Ur\phi_5$ polyhedron, resulting in a flexible framework that can accommodate X^{6+} cations of various sizes.

The structures of $(UO_2)(MoO_4)(H_2O)_2$, $Sr(UO_2)_6(MoO_4)_7(H_2O)_{19}$, $Ba(UO_2)_3(MoO_4)(H_2O)_4$ and $Mg(UO_2)_3(MoO_4)_4(H_2O)_8$ are all frameworks of corner-sharing $Ur\phi_5$ polyhedra and $Mo^{6+}O_4$ tetrahedra (Figs. 13l, m, n, o). In the structure of $(UO_2)(MoO_4)(H_2O)_2$ (Fig. 13l), each $Mo^{6+}O_4$ tetrahedron shares each of its anions with $Ur\phi_5$ polyhedra. The O_{Ur} atoms are only [1]-connected, but four of the equatorial anions of the $Ur\phi_5$ polyhedra are shared with $Mo^{6+}O_4$ tetrahedra, and the remaining anion is an H_2O group. In the structure of $Sr(UO_2)_6(MoO_4)_7(H_2O)_{19}$ (Fig. 13m), the $Mo^{6+}O_4$ tetrahedra share each of their anions with $Ur\phi_5$ polyhedra. There are three symmetrically distinct $Ur\phi_5$ polyhedra; all equatorial anions of two of these are shared with $Mo^{6+}O_4$ tetrahedra, and in the third $Ur\phi_5$ polyhedron, four anions are shared with $Mo^{6+}O_4$ tetrahedra, and the fifth is an H_2O group. In each $Ur\phi_5$ polyhedron, the O_{Ur} atoms are bonded to only the U^{6+} cation. Corner-sharing dimers of $Sr\phi_6$ polyhedra are hydrogen-bonded into the framework. There are three symmetrically distinct $Ur\phi_5$ polyhedra in the structure of $Ba(UO_2)_3(MoO_4)(H_2O)_4$ (Fig. 13n); two of these share all five equatorial anions with $Mo^{6+}O_4$ tetrahedra, the third anion shares four equatorial anions with $Mo^{6+}O_4$ tetrahedra, and the fifth anion is an H_2O group. The Ba cation is coordinated by six oxygen atoms, two of which are also bonded to $Mo^{6+}O_4$ tetrahedra, and the other four are O_{Ur} atoms. The structure of $Mg(UO_2)_3(MoO_4)_4(H_2O)_8$ (Fig. 13o) contains two symmetrically distinct $Ur\phi_5$ polyhedra; in each case, the O_{Ur} atoms bond to only one cation, and all but one of the equatorial anions are shared with $Mo^{6+}O_4$ tetrahedra, with the remaining anion being an H_2O group. The Mg cation is octahedrally coordinated by four H_2O groups and two oxygen atoms; the latter are shared with $Mo^{6+}O_4$ tetrahedra.

The structure of $U^{4+}(UO_2)(PO_4)_2$ contains both U^{4+} and U^{6+}. The U(1) position is coordinated by seven atoms of oxygen, with U–O bond-lengths ranging from 2.17 to 2.54 Å, indicating that the cation is U^{4+} (Bénard *et al.* 1994). The U(2) position is U^{6+}, and the coordination is the usual $Ur\phi_5$ polyhedron. The $U(1)O_7$ and $Ur(2)\phi_5$ polyhedra share edges, giving chains that are cross-linked into a framework by sharing edges and corners with PO_4 tetrahedra (Fig. 13p).

The structure of $Na_2(UO_2)(P_2O_7)$ (Fig. 13q) consists of a framework of corner-sharing $Ur\phi_5$ polyhedra and PO_4 tetrahedra. Each of the equatorial anions of the $Ur\phi_5$ polyhedron are shared with PO_4 tetrahedra, which occur as P_2O_7 pyrophosphate groups. The Na cations are located in voids within the framework, where both symmetrically distinct Na sites are coordinated by seven anions. The O_{Ur} atoms of the uranyl ion are directed toward the Na cations. The uranyl ion U–O(1) and U–O(2) bond-lengths are 1.76 and 1.87 Å, respectively, and the O(1) anion bonds to one Na cation, whereas the O(2) anion is bonded to three Na cations. Also, each equatorial anion of the $Ur\phi_5$ polyhedron is bonded to either one or two Na cations.

Soddyite and $(UO_2)_2(GeO_4)(H_2O)_2$ are isostructural. The structures (Fig. 13r) contain both $Ur\phi_5$ polyhedra and $X^{4+}O_4$ tetrahedra. The $Ur\phi_5$ polyhedra share edges to form chains identical to the chain shown in Figure 11b, and these chains are cross-linked by sharing edges with $X^{4+}O_4$ tetrahedra to chains above and below, resulting in a framework structure.

The structure of $Pb_2(UO_2)(TeO_3)_3$ (Fig. 13s) contains $Ur\phi_5$ polyhedra which corner- and edge-share with $Te^{4+}\phi_n$ polyhedra to form a framework. There are three symmetrically distinct Te^{4+} sites; each bonds to three oxygen atoms at ~1.9 Å; owing to the lone-pair of electrons on the Te^{4+} cation, there are additional bonds to anions at ~2.9 Å. The two symmetrically distinct Pb cations occupy voids in the framework and are coordinated by six and seven oxygen atoms.

The structure of weeksite (Fig. 13t) contains chains of edge-sharing $Ur\phi_5$ polyhedra that share edges with SiO_4 tetrahedra. Adjacent uranyl–silicate chains are linked through (disordered) SiO_4 tetrahedra to form sheets, which are in turn linked into a framework through SiO_4 tetrahedra.

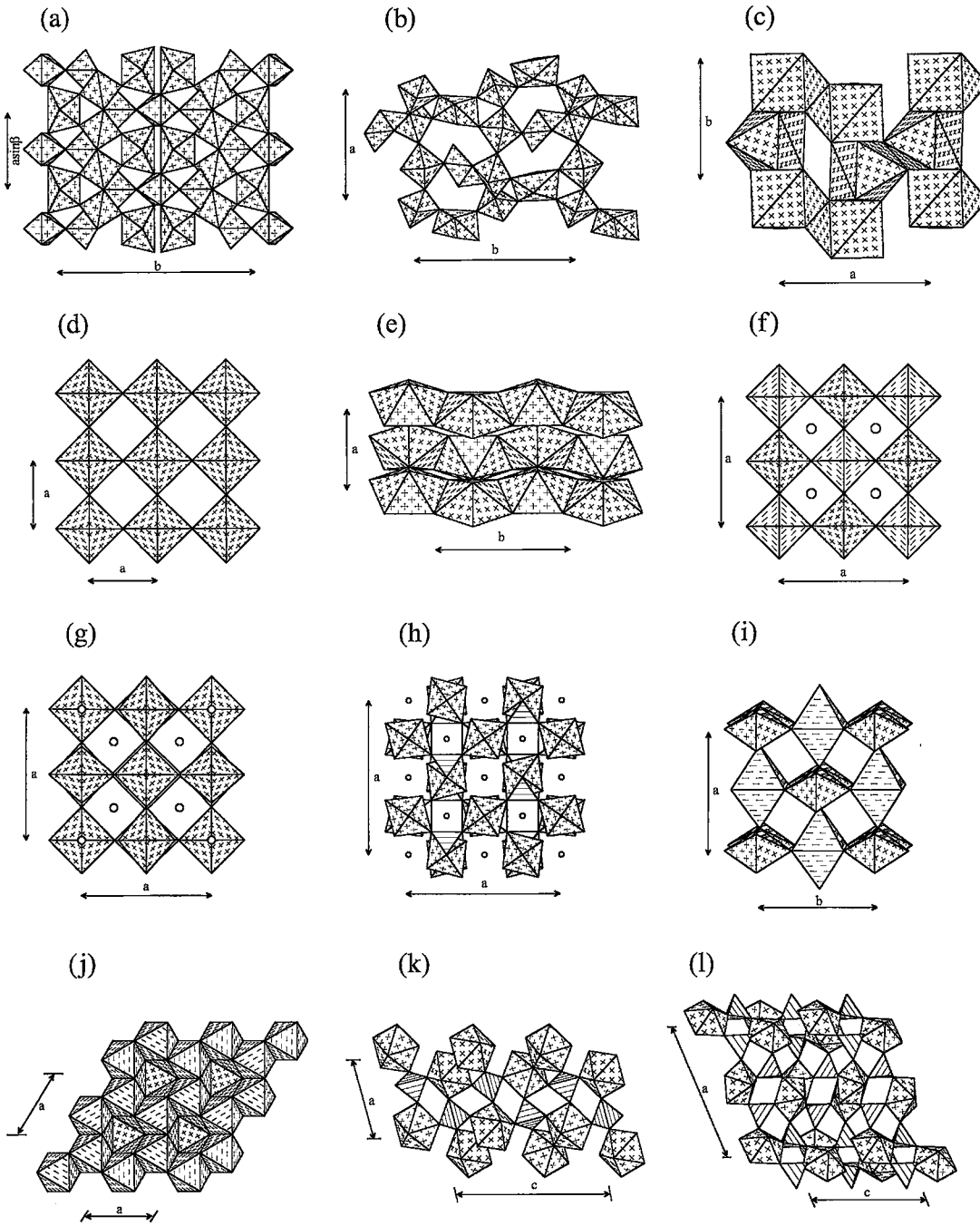

Structures containing $Ur\phi_6$ polyhedra and other cation polyhedra

The structure of synthetic cliffordite (Fig. 13u) is the only framework structure that contains $Ur\phi_6$ polyhedra. There are two symmetrically distinct $Ur\phi_6$ polyhedra. In each case, the O_{Ur} atoms are only [1]-connected, and each equatorial anion is bonded to two Te^{4+} cations. The lone-pair stereoactive Te^{4+} cation is coordinated by five anions in a distorted

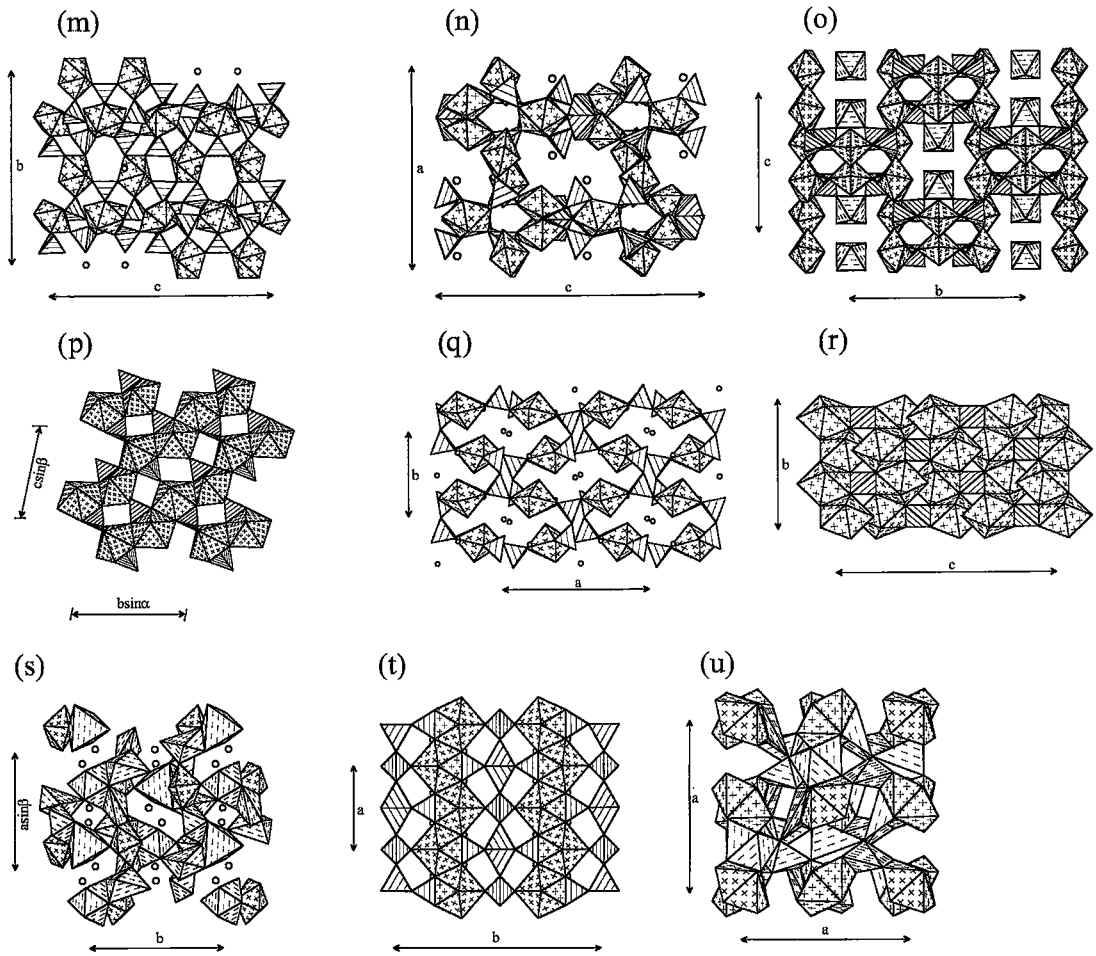

FIG. 13. Structures that are frameworks of polyhedra. The corresponding structures are listed in Table 9. Legend as in Figure 3, except that low-valence cations are shown as open circles, and non-U^{6+} octahedra are shaded with broken lines.

square-pyramidal geometry.

SUMMARY

A total of 180 crystal structures that contain U^{6+} have been placed in a hierarchy of structures that is based upon the polymerization of cation polyhedra of higher bond-valence. Of these, fifty-six are known as minerals. Although structures with sheets, chains, isolated clusters, isolated polyhedra and frameworks all occur, the majority of the phases that contain U^{6+} adopt sheet structures. Of all structures that contain U^{6+}, 59% are based on sheets, and 77% of the minerals have structures based upon sheets of polyhedra.

One hundred and six uranyl phases adopt sheet structures, and there are almost as many distinct sheets. The sheets have been classified on the basis of details of the underlying anion-topology; twenty-nine anion-topologies are defined. In several cases, a sheet that gives rise to a unique anion-topology occurs in only one structure. Only six anion-topologies are required to describe the sheets that occur in 83% of sheet structures (60% in the case of minerals). These are the uranophane, francevillite, autunite, protasite, phosphuranylite, and α-UO_3 anion-topologies. We are currently investigating the origin of this preference.

Various cations, including low-valence cations (*i.e.*, Pb, Ca, Na, Cu), can occur within the sheets in these phases; they occupy sites that commonly are remarkably similar to those occupied by U^{6+}. Also, there are many sites in a given anion-topology that are vacant in the corresponding sheets, and these sites

are potential locations for minor amounts of low-valence cations, assuming that appropriate charge-balance mechanisms are possible. This finding suggests that limited solid-solution may occur in many of these structures, and this has significant implications both in mineralogy, and in the accommodation of radionuclides in these structures, where these phases occur as the corrosion products of the UO_2 in spent nuclear fuel.

Acknowledgements

This work was supported by the Natural Sciences and Engineering Research Council of Canada in the form of a Post-Doctoral Fellowship to PCB and by the Office of Basic Energy Sciences (Grant No. DE–FG03–95ER14540). Kate Helean assisted with the preparation of the preliminary structure-drawings. We thank Professor R.H. Doremus for his comments on an earlier version of this manuscript. This manuscript was substantially improved following a detailed review by Dr. Robert Finch. The clarity of this contribution was improved by the editorial work of Dr. Robert F. Martin.

References

Åberg, M. (1969): The crystal structure of $[(UO_2)_2(OH)_2Cl_2(H_2O)_4]$. *Acta Chem. Scand.* **23**, 791-810.

_____ (1976): The crystal structure of $[(UO_2)_4Cl_2O_2(OH)_2(H_2O)_6]\cdot 4H_2O$, a compound containing a tetranuclear aquachlorohydroxooxo complex of uranyl(VI). *Acta Chem. Scand.* **A30**, 507-514.

_____ (1978): The crystal structure of hexaaqua-tri-μ-hydroxo-μ_3-oxo-triuranyl(VI) nitrate tetrahydrate, $[(UO_2)_3O(OH)_3(H_2O)_6]NO_3\cdot 4H_2O$. *Acta Chem. Scand.* **A32**, 101-107.

Alcock, N.W., Roberts, M.M. & Brown, D. (1982): Actinide structural studies. 3. The crystal and molecular structures of $UO_2SO_4\cdot H_2SO_4\cdot 5H_2O$ and $(NpO_2SO_4)_2\cdot H_2SO_4\cdot 4H_2O$. *J. Chem. Soc., Dalton Trans.* **1982**, 869-873.

Allpress, J.G. & Wadsley, A.D. (1964): The crystal structure of caesium uranyl oxychloride $Cs_{0.9}(UO_2)OCl_{0.9}$. *Acta Crystallogr.* **17**, 41-46.

Appleman, D.E. & Evans, H.T., Jr. (1965): The crystal structures of synthetic anhydrous carnotite, $K_2(UO_2)_2V_2O_8$, and its cesium analogue, $Cs_2(UO_2)_2V_2O_8$. *Am. Mineral.* **50**, 825-842.

Atencio, D., Neumann, R., Silva, A.J.G.C. & Mascarenhas, Y.P. (1991): Phurcalite from Perus, São Paulo, Brazil, and redetermination of its crystal structure. *Can. Mineral.* **29**, 95-105.

Bachet, B., Brassy, C. & Cousson, A. (1991): Structure de $Mg((UO_2)(AsO_4))_2\cdot 4H_2O$. *Acta Crystallogr.* **C47**, 2013-2015.

Bacmann, M. & Bertaut, E.F. (1966): Paramètres atomiques et structure magnétique de $MnUO_4$. *J. Physique* **27**, 726-734.

Baturin, S.V. & Sidorenko, G.A. (1985): Crystal structure of weeksite $(K_{.62}Na_{.38})_2(UO_2)_2[Si_5O_{13}]\cdot 3H_2O$. *Dokl. Akad. Nauk SSSR* **282**, 1132-1136 (in Russ.).

Behm, H. (1985): Hexpotassium(cyclo-octahydroxotetracosaoxohexadecaborato) dioxouranate(VI) dodecahyrate, $K_6[UO_2\{B_{16}O_{24}(OH)_8\}]\cdot 12H_2O$. *Acta Crystallogr.* **C41**, 642-645.

Bénard, P., Louër, D., Dacheux, N., Brandel, V. & Genet, M. (1994): $U(UO_2)(PO_4)_2$, a new mixed-valence uranium orthophosphate: *ab initio* structure determination from powder diffraction data and optical and X-ray photoelectron spectra. *Chem. Mater.* **6**, 1049-1058.

Birch, W.D., Mumme, W.G. & Segnit, E.R. (1988): Ulrichite: a new copper calcium uranium phosphate from Lake Boga, Victoria, Australia. *Aust. Mineral.* **3**, 125-131.

Blatov, V.A., Serezhkina, L.B., Serezkhin, L.B. & Trunov, V.K. (1989): Crystal structure of $NH_4UO_2SeO_4F\cdot H_2O$. *Zh. Neorg. Khim.* **34**, 162-164 (in Russ.).

Borène, J. & Cesbron, F. (1970): Structure cristalline de l'uranyl-vanadate de nickel tétrahydraté $Ni(UO_2)_2(VO_4)_2\cdot 4H_2O$. *Bull. Soc. fr. Minéral. Cristallogr.* **93**, 426-432.

_____ & _____ (1971): Structure cristalline de la curiénite $Pb(UO_2)_2(VO_4)_2\cdot 5H_2O$. *Bull. Soc. fr. Minéral. Cristallogr.* **94**, 8-14.

Bragg, W.L. (1930): The structure of silicates. *Z. Kristallogr.* **74**, 237-305.

Brandenburg, N.P. & Loopstra, B.O. (1973): Uranyl sulphate hydrate, $UO_2SO_4\cdot 3\frac{1}{2}H_2O$. *Cryst. Struct. Commun.* **2**, 243-246.

_____ & _____ (1978): β-uranyl sulphate and uranyl selenate. *Acta Crystallogr.* **B34**, 3734-3736.

Branstätter, F. (1981a): Synthesis and crystal structure determination of $Pb_2(UO_2)((TeO_3)_3)$. *Z. Kristallogr.* **155**, 193-200.

_____ (1981b): Non-stoichiometric, hydrothermally synthesized cliffordite. *Tschermaks Mineral. Petrogr. Mitt.* **29**, 1-8.

Brown, I.D. (1981): The bond-valence method: an empirical approach to chemical structure and bonding. *In* Structure and Bonding in Crystals II (M. O'Keeffe & A. Navrotsky, eds.). Academic Press, New York, N.Y. (1-30).

Burns, P.C., Grice, J.D. & Hawthorne, F.C. (1995): Borate minerals. I. Polyhedral clusters and fundamental building blocks. *Can. Mineral.* **33**, 1131-1151.

CHEVALIER, R. & GASPERIN, M. (1968): Structure cristalline de l'oxyde double UNb_3O_{10}. *C.R. Acad. Sci. Paris* **C267**, 481-483.

_____ & _____ (1969): Synthèse en monocristaux et structure cristalline de l'oxyde $UTiNb_2O_{10}$. *C.R. Acad. Sci. Paris* **C268**, 1426-1428.

CHRIST, C.L., CLARK, J.R. & EVANS, H.T., JR. (1955): Crystal structure of rutherfordine, UO_2CO_3. *Science* **121**, 472-473.

COOPER, M.A. & HAWTHORNE, F.C. (1995): The crystal structure of guilleminite, a hydrated Ba–U–Se sheet structure. *Can. Mineral.* **33**, 1103-1109.

CORDFUNKE, E.H.P., VAN VLAANDERSEN, P., ONINK, M. & IJDO, D.J.W. (1991): $Sr_3U_{11}O_{36}$: crystal structure and thermal stability. *J. Solid State Chem.* **94**, 12-18.

CREMERS, T.L., ELLER, P.G., LARSON, E.M. & ROSENZWEIG, A. (1986): Single-crystal structure of lead uranate(VI). *Acta Crystallogr.* **C42**, 1684-1685.

DALLEY, N.K., MUELLER, M.H. & SIMONSEN, S.H. (1971): A neutron diffraction study of uranyl nitrate dihydrate. *Inorg. Chem.* **10**, 323-328.

DEBETS, P.C. (1966): The structure of β-UO_3. *Acta Crystallogr.* **21**, 589-593.

_____ (1968): The structures of uranyl chloride and its hydrates. *Acta Crystallogr.* **B24**, 400-402.

DEMARTIN, F., DIELLA, V., DONZELLI, S., GRAMACCIOLI, C.M. & PILATI, T. (1991): The importance of accurate crystal structure determination of uranium minerals. I. Phosphuranylite $KCa(H_3O)_3(UO_2)_7(PO_4)_4O_4{\cdot}8H_2O$. *Acta Crystallogr.* **B47**, 439-446.

_____, GRAMACCIOLI, C.M. & PILATI, T. (1992): The importance of accurate crystal structure determination of uranium minerals. II. Soddyite $(UO_2)_2(SiO_4){\cdot}2H_2O$. *Acta Crystallogr.* **C48**, 1-4.

DICKENS, P.G., STUTTARD, G.P., BALL, R.G.J., POWELL, A.V., HULL, S. & PATAT, S. (1992): Powder neutron diffraction study of the mixed uraniumvanadium oxides $Cs_2(UO_2)_2(V_2O_8)$ and UVO_5. *J. Mater. Chem.* **2**, 161-166.

_____, _____ & PATAT, S. (1993): Structure of CuU_3O_{10}. *J. Mater. Chem.* **3**, 339-341.

EVANS, H.T., JR. (1963): Uranyl ion coordination. *Science* **141**, 154-157.

FINCH, R.J. & EWING, R.C. (1992): The corrosion of uraninite under oxidizing conditions. *J. Nucl. Mater.* **190**, 133-156.

_____, COOPER, M.A., HAWTHORNE, F.C. & EWING, R.C. (1996): The crystal structure of schoepite, $[(UO_2)_8O_2(OH)_{12}](H_2O)_{12}$. *Can. Mineral.* **34**, (in press).

FITCH, A.N., BERNARD, L., HOWE, A.T., WRIGHT, A.F. & FENDER, B.E.F. (1983): The room-temperature structure of $DUO_2AsO_5{\cdot}4D_2O$ by powder neutron diffraction. *Acta Crystallogr.* **C39**, 159-162.

_____ & COLE, M. (1991): The structure of $KUO_2PO_4{\cdot}3D_2O$ refined from neutron and synchrotron-radiation powder diffraction data. *Mater. Res. Bull.* **26**, 407-414.

_____ & FENDER, B.E.F. (1983): The structure of deuterated ammonium uranyl phosphate trihydrate, $ND_4UO_2PO_4{\cdot}3D_2O$ by powder neutron diffraction. *Acta Crystallogr.* **C39**, 162-166.

_____, _____ & WRIGHT, A.F. (1982): The structure of deuterated lithium uranyl arsenate tetrahydrate $LiUO_2AsO_4{\cdot}4D_2O$ by powder neutron diffraction. *Acta Crystallogr.* **B38**, 1108-1112.

FLEISCHER, M. & MANDARINO, J.A. (1991): *Glossary of Mineral Species 1991*. The Mineralogical Record Inc., Tucson, Arizona, U.S.A.

FUJINO, T., MASAKI, N. & TAGAWA, H. (1977): The crystal structures of α- and γ-$SrUO_4$. *Z. Kristallogr. Kristallgeom. Kristallphys. Kristallchem.* **145**, 299-309.

GASPERIN, M. (1987a): Synthèse et structure du diborouranate de magnésium, MgB_2UO_7. *Acta Crystallogr.* **C43**, 2264-2266.

_____ (1987b): Synthèse et structure de trois niobo-uranates d'ions monovalents: $TlNb_2U_2O_{11.5}$, $KNbUO_6$, et $RbNbUO_6$. *J. Solid State Chem.* **67**, 219-224.

_____ (1987c): Synthèse et structure du niobouranate de césium: $CsNbUO_6$. *Acta Crystallogr.* **C43**, 404-406.

_____ (1987d): Synthèse et structure du borouranate de calcium: $CaB_2U_2O_{10}$. *Acta Crystallogr.* **C43**, 1247-1250.

_____ (1987e): Structure du borate d'uranium UB_2O_6. *Acta Crystallogr.* **C43**, 2031-2033.

_____ (1988): Synthèse et structure du borouranate de sodium, $NaBUO_5$. *Acta Crystallogr.* **C44**, 415-416.

_____ (1990): Synthèse et structure du borouranate de lithium $LiBUO_5$. *Acta Crystallogr.* **C46**, 372-374.

_____, REBIZANT, J., DANCAUSSE, J.P., MEYER, D. & COUSSON, A. (1991): Structure de $K_9BiU_6O_{24}$. *Acta Crystallogr.* **C47**, 2278-2279.

GEBERT, E., HOEKSTRA, H.R., REIS, A.H. JR & PETERSON, S.W. (1978): The crystal structure of lithium uranate. *J. Inorg. Nucl. Chem.* **40**, 65-68.

GINDEROW, D. (1988): Structure de l'uranophane alpha, $Ca(UO_2)_2(SiO_3OH)_2{\cdot}5H_2O$. *Acta Crystallogr.* **C44**, 421-424.

_____ & CESBRON, F. (1983a): Structure de la derriksite, $Cu_4(UO_2)(SeO_3)_2(OH)_6$. *Acta Crystallogr.* **C39**, 1605-1607.

_____ & _____ (1983b): Structure de la demesmaekerite, $Pb_2Cu_5(SeO_3)_6(UO_2)_2(OH)_6{\cdot}2H_2O$. *Acta Crystallogr.* **C39**, 824-827.

_____ & _____ (1985): Structure de la roubaultite, $Cu_2(UO_2)_3(CO_3)_2O_2(OH)_2{\cdot}4H_2O$. *Acta Crystallogr.* **C41**, 654-657.

GORBUNOVA, YU.E., LINDE, S.A., LAVROV, A.V. & POBEDINA, A.B. (1980): Synthesis and structure of $Na_{6-x}(UO_2)_3(H_xPO_4)(PO_4)_3$ (x = 0.5). *Dokl. Akad. Nauk SSSR* **251**, 385-389 (in Russ.).

HANIC, F. (1960): The crystal structure of meta-zeunerite $Cu(UO_2)_2(AsO_4)_2{\cdot}8H_2O$. *Czech. J. Phys.* **10**, 169-181.

HAWTHORNE, F.C. (1983): Graphical enumeration of polyhedral clusters. *Acta Crystallogr.* **A39**, 724-736.

_____ (1985): Towards a structural classification of minerals: the $^{vi}M^{iv}T_2\phi_n$ minerals. *Am. Mineral.* **70**, 455-473.

_____ (1990): Structural hierarchy in $M^{[6]}T^{[4]}\phi_n$ minerals. *Z. Kristallogr.* **192**, 1-52.

HOEKSTRA, H.R. & SIEGEL, S. (1971): Preparation and properties of Cr_2UO_6. *J. Inorg. Nucl. Chem.* **33**, 2867-2873.

IJDO, D.J.W. (1993a): $Pb_3U_{11}O_{36}$, a Rietveld refinement of neutron powder diffraction data. *Acta Crystallogr.* **C49**, 654-656.

_____ (1993b): Redetermination of tristrontium uranate (VI). A Rietveld refinement of neutron powder diffraction data. *Acta Crystallogr.* **C49**, 650-652.

JOVE, J., COUSSON, A. & GASPERIN, M. (1988): Synthesis and crystal structure of $K_2U_2O_7$ and Mössbauer (Np-237) studies of $K_2Np_2O_7$ and $CaNpO_4$. *J. Less-Common Metals* **139**, 345-350.

KAPSHUKOV, I.I., VOLKOV, YE.F., MOSKVITSEV, E.P., LEBEDEV, I.A. & YAKOVLEV, G.N. (1971): Crystalline structure of uranyl tetranitrates. *Zh. Struct. Khim.* **12**, 94-98 (in Russ.).

KHOSRAWAN-SAZEDJ, F. (1982a): The crystal structure of meta-uranocircite. II. $Ba(UO_2)_2(PO_4)_2{\cdot}6H_2O$. *Tschermaks Mineral. Petrogr. Mitt.* **29**, 193-204.

_____ (1982b): On the space group of threadgoldite. *Tschermaks Mineral. Petrogr. Mitt.* **30**, 111-115.

KOSTER, A.S., RENAUD, J.P.P. & RIECK, J.D. (1975): The crystal structures at 20 and 1000°C of bismuth uranate, Bi_2UO_6. *Acta Crystallogr.* **B31**, 127-131.

KOVBA, L.M. (1971): The crystal structure of potassium and sodium monouranates. *Radiokhimiya* **13**, 309-311 (in Russ.).

_____ (1972a): Crystal structure of $K_2U_7O_{22}$. *J. Struct. Chem.* **13**, 235-238.

_____ (1972b): Structure of lithium triuranate. *J. Struct. Chem.* **13**, 428-430.

_____, IPPOLITOVA, E.A., SIMANOV, YU.P. & SPITSYN, V.I. (1958): The X-ray investigation of uranates of alkali elements. *Dokl. Akad. Nauk SSSR* **120**, 1042-1044 (in Russ.).

KRAUSE, W., EFFENBERGER, H. & BRANDSTÄTTER, F. (1995): Orthowalpurgite, $(UO_2)Bi_4O_4(AsO_4)_2{\cdot}2H_2O$, a new mineral from the Black Forest, Germany. *Eur. J. Mineral.* **7**, 1313-1324.

KROGH-ANDERSEN, E., KROGH-ANDERSEN, I.G. & PLOUG-SOERENSEN, G. (1985): Structure determination of a substance alleged to be hendecahydrogen diuranyl pentaphosphate. *Solid State Protonic Conduct. Fuel Cells Sens., Eur. Workshop "Solid State Mater. Low Medium Temp. Fuel Cells Monit., Spec. Emphasis Proton Conduct."* (J.B. Goodenough, J. Jensen & A. Potier, eds.). Odense Univ. Press, Odense, Denmark (191-202).

LANGMUIR, D. (1978): Uranium solution – mineral equilibria at low temperatures with applications to sedimentary ore deposits. *Geochim. Cosmochim. Acta* **42**, 547-569.

LEE, M.R. & JAULMES, S. (1987): Nouvelle série d'oxydes dérivés de la structure de α-U_3O_8: M(II) UMo_4O_{16}. *J. Solid State Chem.* **67**, 364-368.

LEGROS, J.P. & JEANNIN, Y. (1975): Coordination de l'uranium par l'ion germanate. II. Structure du germanate d'uranyle dihydraté $(UO_2)_2GeO_4(H_2O)_2$. *Acta Crystallogr.* **B31**, 1140-1143.

LIEBAU, F. (1985): *Structural Chemistry of Silicates.* Springer-Verlag, Berlin, Germany.

LINDE, S.A., GORBUNOVA, Y.E. & LAVROV, A.V. (1980): Crystal structure of $K_4UO_2(PO_4)_2$. *Zh. Neorg. Khim.* **25**, 1992-1994 (in Russ.).

_____, _____, _____ & KUZNETSOV, V.G. (1978): Synthesis and structure of $CsUO_2(PO_3)_3$ crystals. *Dokl. Akad. Nauk SSSR* **242**, 1083-1085 (in Russ.).

_____, _____, _____ & POBEDINA, A.B. (1984): The synthesis and structure of crystals of sodium uranyl pyrophosphate $Na_2UO_2P_2O_7$. *Zh. Neorg. Khim.* **29**, 1533-1537 (in Russ.).

LOOPSTRA, B.O. (1970): The structure of β-U_3O_8. *Acta Crystallogr.* **B26**, 656-657.

_____ (1977): On the crystal structure of α-U_3O_8. *J. Inorg. Nucl. Chem.* **39**, 1713-1714.

_____ & BRANDENBURG, N.P. (1978): Uranyl selenite and uranyl tellurite. *Acta Crystallogr.* **B34**, 1335-1337.

_____ & CORDFUNKE, E.H.P. (1966): On the structure of α-UO_3. *Rec. Trav. Chim. Pays-Bas* **85**, 135-142.

_____ & RIETVELD, H.M. (1969): The structure of some alkaline-earth metal uranates. *Acta Crystallogr.* **B25**, 787-791.

_____, TAYLOR, J.C. & WAUGH, A.B. (1977): Neutron powder profile studies of the gamma uranium trioxide phases. *J. Solid State Chem.* **20**, 9-19.

MAKAROV, Y.S. & ANIKINA, L.I. (1963): Crystal structure of umohoite $(UMoO_6(H_2O)_2)\cdot 2H_2O$. *Geochemistry*, 14-21.

_____ & IVANOV, V.I. (1960): The crystal structure of meta-autunite, $Ca(UO_2)_2(PO_4)_2\cdot 6H_2O$. *Dokl. Acad. Sci. USSR, Earth Sci. Sect.* **132**, 601-603.

MAYER, H. & MEREITER, K. (1986): Synthetic bayleyite, $Mg_2[UO_2(CO_3)_3]\cdot 18H_2O$: thermochemistry, crystallography and crystal structure. *Tschermaks Mineral. Petrogr. Mitt.* **35**, 133-146.

MEREITER, K. (1982a): The crystal structure of liebigite, $Ca_2UO_2(CO_3)_3\approx 11H_2O$. *Tschermaks Mineral. Petrogr. Mitt.* **30**, 277-288.

_____ (1982b): The crystal structure of walpurgite, $(UO_2)Bi_4O_4(AsO_4)_2\cdot 2H_2O$. *Tschermaks Mineral. Petrogr. Mitt.* **30**, 129-139.

_____ (1982c): Die Kristallstruktur des Johannits, $Cu(UO_2)_2(OH)_2(SO_4)_2\cdot 8H_2O$. *Tschermaks Mineral. Petrogr. Mitt.* **30**, 47-57.

_____ (1986a): Crystal structure and crystallographic properties of a schröckingerite from Joachimsthal. *Tschermaks Mineral. Petrogr. Mitt.* **35**, 1-18.

_____ (1986b): Synthetic swartzite, $CaMg[UO_2(CO_3)_3]\cdot 12H_2O$, and its strontium analogue, $SrMg[UO_2(CO_3)_3]\cdot 12H_2O$: crystallography and crystal structures. *Neues Jahrb. Mineral., Monatsh.*, 481-492.

_____ (1986c): Neue kristallographische Daten ueber das Uranmineral Andersonit. *Anz. Oesterr. Akad. Wiss. Math.-Naturwiss. Kl.* **3**, 39-41.

_____ (1986d): Structure of strontium tricarbonatodioxouranate(VI) octahydrate. *Acta Crystallogr.* **C42**, 1678-1681.

_____ (1986e): Crystal structure refinements of two francevillites, $(Ba,Pb)[(UO_2)_2V_2O_8]\cdot 5H_2O$. *Neues Jahrb. Mineral., Monatsh.*, 552-560.

_____ (1988): Structure of caesium tricarbonatodioxouranate(VI) hexahydrate. *Acta Crystallogr.* **C44**, 1175-1178.

MEUNIER, G. & GALY, J. (1973): Structure cristalline de la schmitterite synthétique $UTeO_5$. *Acta Crystallogr.* **B29**, 1251-1255.

MIJLHOFF, F.C., IIDO, D.J.W. & CORDFUNKE, E.H.P. (1993): The crystal structure of α- and β-$Cs_2U_2O_7$. *J. Solid State Chem.* **102**, 299-305.

MILLER, M.L., FINCH, R.J., BURNS, P.C. & EWING, R.C. (1995): Description and classification of uranium oxide hydrate sheet topologies. *In* The Scientific Basis for Nuclear Waste Management XIX (W.M. Murphy & D.A. Knecht, eds.). *Materials Research Soc., Proc.* **412**, 369-376.

_____, _____ , _____ & _____ (1996): Description and classification of uranium oxide hydrate sheet topologies. *J. Mater. Res.* (in press).

MILLER, S.A. & TAYLOR, J.C. (1986): The crystal structure of saleeite, $Mg[UO_2PO_4]_2\cdot 10H_2O$. *Z. Kristallogr.* **177**, 247-253.

MISTRYUKOV, V.E. & MICHAILOV, Y.N. (1983): The characteristic properties of the structural function of the selenitogroup in the uranyl complex with neutral ligands. *Koord. Khim.* **9**, 97-102 (in Russ.).

MOORE, P.B. (1965): A structural classification of Fe–Mn orthophosphate hydrates. *Am. Mineral.* **50**, 2052-2062.

_____ (1973): Pegmatite phosphates: descriptive mineralogy and crystal chemistry. *Mineral. Rec.* **4**, 103-130.

MOROSIN, B. (1978): Hydrogen uranyl tetrahydrate, a hydrogen ion solid electrolyte. *Acta Crystallogr.* **B34**, 3732-3734.

MURPHY, W.M. & PABALAN, R.T. (1995): Review of empirical thermodynamic data for uranyl silicate minerals and experimental plan. *Center for Nuclear Waste Regulatory Analyses, Rep.* **95-014**.

NIINISTÖ, L., TOIVONEN, J. & VALKONEN, J. (1978): Uranyl (VI) compounds. I. The crystal structure of ammonium uranyl sulfate dihydrate, $(NH_4)_2UO_2(SO_4)_2\cdot 2H_2O$. *Acta Chem. Scand.* **A32**, 647-651.

_____, _____ & _____ (1979): Uranyl (VI) compounds. II. The crystal structure of potassium uranyl sulfate dihydrate, $K_2UO_2(SO_4)_2\cdot 2H_2O$. *Acta Chem. Scand.* **A33**, 621-624.

PADEL, L., POIX, P. & MICHEL, A. (1972): Préparation et étude cristallographique du système $Ba_2(UMg)O_6$ – $Ba_2(U_{2/3}Fe_{4/3})O_6$. *Rev. Chim. Minérale* **9**, 337-350.

PAGOAGA, M.K., APPLEMAN, D.E. & STEWART, J.M. (1987): Crystal structures and crystal chemistry of the uranyl oxide hydrates becquerelite, billietite, and protasite. *Am. Mineral.* **72**, 1230-1238.

PERRIN, A. (1976): Structure cristalline du nitrate de dihydroxo diuranyle tétrahydraté. *Acta Crystallogr.* **B32**, 1658-1661.

_____ (1977): Préparation, étude structurale et vibrationnelle des complexes $M_2U_2O_5Cl_4{\cdot}2H_2O$ (M = Rb, Cs): mise en evidence d'un anion tétranucléaire $[(UO_2)_4O_2Cl_8(H_2O)_2]^{4-}$. *J. Inorg. Nucl. Chem.* **39**, 1169-1172.

_____ & LE MAROUILLE, J.Y. (1977): Structure cristalline et moléculaire du complexe tétranucléaire $K_2(UO_2)_4O_2(OH)_2Cl_4(H_2O)_6$. *Acta Crystallogr.* **B33**, 2477-2481.

PIRET, P. (1985): Structure cristalline de la fourmariérite, $Pb(UO_2)_4O_3(OH)_4{\cdot}4H_2O$. *Bull. Minéral.* **108**, 659-665.

_____ & DECLERCQ, J.-P. (1983): Structure cristalline de l'upalite $Al[(UO_2)_3O(OH)(PO_4)_2]{\cdot}7H_2O$. Un exemple de macle mimétique. *Bull. Minéral.* **106**, 383-389.

_____, _____ & WAUTERS-STOOP, D. (1980): Structure cristalline de la sengiérite. *Bull. Minéral.* **103**, 176-178.

_____ & DELIENS, M. (1982): La vanmeersscheite $U(UO_2)_3(PO_4)_2(OH)_6{\cdot}4H_2O$ et la méta-vanmeersscheite $U(UO_2)_3(PO_4)_2(OH)_6{\cdot}2H_2O$, nouveaux minéraux. *Bull. Minéral.* **105**, 125-128.

_____ & _____ (1987): Les phosphates d'uranyle et d'aluminium de Kobokobo. IX. L'althupite $AlTh(UO_2)[(UO_2)_3O(OH)(PO_4)_2]_2(OH)_3{\cdot}15H_2O$, nouveau minéral; propriétés et structure cristalline. *Bull. Minéral.* **110**, 65-72.

_____, _____ & PIRET-MEUNIER, J. (1988): La françoisite-(Nd), nouveau phosphate d'uranyle et de terres rares; propriétés et structure cristalline. *Bull. Minéral.* **111**, 443-449.

_____, _____, _____ & GERMAIN, G. (1983): La sayrite, $Pb_2[(UO_2)_5O_6(OH)_2]{\cdot}4H_2O$. Nouveau minéral; propriétés et structure cristalline. *Bull. Minéral.* **106**, 299-304.

_____ & PIRET-MEUNIER, J. (1988): Nouvelle détermination de la structure cristalline de la dumontite $Pb_2[(UO_2)_3O_2(PO_4)_2]{\cdot}5H_2O$. *Bull. Minéral.* **111**, 439-442.

_____, _____ & DECLERCQ, J.-P. (1979): Structure of phuralumite. *Acta Crystallogr.* **B35**, 1880-1882.

_____, _____ & DELIENS, M. (1990): Composition chimique et structure cristalline de la dewindtite $Pb_3[H(UO_2)_3O_2(PO_4)_2]_2{\cdot}12H_2O$. *Eur. J. Mineral.* **2**, 399-405.

REIS, A.H., JR., HOEKSTRA, H.R., GEBERT, E. & PETERSON, S.W. (1976): Redetermination of the crystal structure of barium uranate. *J. Inorg. Nucl. Chem.* **38**, 1481-1485.

RESHETOV, K.V. & KOVBA, L.M. (1966): Structures of $SrUO_{(4-x)}$, $CdUO_{(4-x)}$ and Li_4UO_5. *J. Struct. Chem.* **7**, 589-590.

ROSENZWEIG, A. & RYAN, R.R. (1975): Refinement of the crystal structure of cuprosklodowskite, $Cu[(UO_2)_2(SiO_3OH)_2]{\cdot}6H_2O$. *Am. Mineral.* **60**, 448-453.

_____ & _____ (1977a): Kasolite, $Pb(UO_2)(SiO_4){\cdot}H_2O$. *Cryst. Struct. Commun.* **6**, 617-621.

_____ & _____ (1977b): Vandenbrandeite $Cu(UO_2)(OH)_4$. *Cryst. Struct. Commun.* **6**, 53-56.

ROSS, M. & EVANS, H.T., JR. (1960): The crystal structure of cesium biuranyl trisulfate, $Cs_2(UO_2)_2(SO_4)_3$. *J. Inorg. Nucl. Chem.* **15**, 338-351.

_____ & _____ (1964): Studies of the torbernite minerals. I. The crystal structure of abernathyite and the structurally related compounds $NH_4(UO_2AsO_4){\cdot}3H_2O$ and $K(H_3O)(UO_2AsO_4)_2{\cdot}6H_2O$. *Am. Mineral.* **49**, 1578-1602.

RYAN, R.R. & ROSENZWEIG, A. (1977): Sklodowskite, $MgO{\cdot}2UO_3{\cdot}2SiO_2{\cdot}7H_2O$. *Cryst. Struct. Commun.* **6**, 611-615.

SADIKOV, G.G., KRASOVSKAYA, T.I., POLYAKOV, Y.A. & NIKOLAEV, V.P. (1988): Structural and spectral studies on potassium dimolybdatouranylate. *Inorg. Mater.* **24**, 91-96.

SAINE, M.C. (1989): Synthèse et structure de KU_2O_7 monoclinique. *J. Less-Common Metals* **154**, 361-365.

SARIN, V.A., LINDE, S.A., FIKIN, L.E., DUDAREV, V.YA. & GORBUNOVA, Y.E. (1983): Neutronographic study of $UO_2H(PO_3)_3$ monocrystals. *Zh. Neorg. Khim.* **28**, 1538-1541 (in Russ.).

SEREZHKIN, V.N., BOIKO, N.V. & TRUNOV, V.K. (1982): The crystal structure of $Sr[UO_2(OH)CrO_4]_2{\cdot}8H_2O$. *Zh. Strukt. Khim.* **23**, 270-273 (in Russ.).

_____, CHUVAEV, V.F., KOVBA, L.M. & TRUNOV, V.K. (1973): The structure of synthetic iriginite. *Dokl. Akad. Nauk SSSR* **210**, 873-876 (in Russ.).

_____, EFREMOV, V.A. & TRUNOV, V.K. (1980b): The crystal structure of $\alpha UO_2MoO_4{\cdot}H_2O$. *Kristallografiya* **25**, 861-865 (in Russ.).

_____, SOLDATKINA, M.A. & BOIKO, N.V. (1983): The refinement of the crystal structure $(NH_4)_4[UO_2(CO_3)_3]$. *J. Struct. Chem.* **24**, 770-774.

_____, _____ & EFREMOV, V.A. (1981a): Crystal structure of the uranyl selenate tetrahydrate. *J. Struct. Chem.* **22**, 451-454.

_____, _____ & _____ (1981b): Crystal structure of $MgUO_2(SO_4)_2{\cdot}11H_2O$. *J. Struct. Chem.* **22**, 454-457.

_____ & TRUNOV, V.K. (1981): The crystal structure of $UO_2CrO_4{\cdot}5.5H_2O$. *Kristallografiya* **26**, 301-304 (in Russ.).

_____, _____ & MAKAREVICH, L.G. (1980a): The refined crystal structure of uranyl molybdate. *Kristallografiya* **25**, 858-860 (in Russ.).

SEREZHKINA, L.B., TRUNOV, V.K., KHOLODKOVSKAYA, L.N. & KUCHUMOVA, N.V. (1990): Crystal structure of $K[UO_2CrO_4(OH)]\cdot 1.5H_2O$. *Koord. Khim.* **16**, 1288-1291 (in Russ.).

SHASHKIN, D.P., LUR'E, E.A. & BELOV, N.V. (1974): Crystal structure of $Na_2[(UO_2)SiO_4]$. *Kristallografiya* **19**, 958-963 (in Russ.).

SIEGEL, S. & HOEKSTRA, H.R. (1968): The crystal structure of copper uranium tetroxide. *Acta Crystallogr.* **B24**, 967-970.

———, ——— & GEBERT, E. (1972b): The structure of γ-uranyl dihydroxide, $UO_2(OH)_2$. *Acta Crystallogr.* **B28**, 3469-3473.

———. ——— & SHERRY, E. (1966): The crystal structure of high-pressure UO_3. *Acta Crystallogr.* **20**, 292-295.

———, VISTE, A., HOEKSTRA, H.R. & TANI, B.S. (1972a): The structure of hydrogen triuranate. *Acta Crystallogr.* **B28**, 117-121.

SMITH, D.K. (1984): Uranium mineralogy. *In* Uranium Geochemistry, Mineralogy, Geology, Exploration and Resources (F. Ippolito, B. DeVero & G. Capaldi, eds.). Institution of Mining and Metallurgy, London, U.K.

STERGIOU, A.C., RENTZEPERIS, P.J. & SKLAVOUNOS, S. (1993): Refinement of the crystal structure of metatorbernite. *Z. Kristallogr.* **205**, 1-7.

STERNS, M., PARISE, J.B. & HOWARD, C.J. (1986): Refinement of the structure of trilead(II) uranate(VI) from neutron powder diffraction data. *Acta Crystallogr.* **C42**, 1275-1277.

STOHL, F.V. & SMITH, D.K. (1981): The crystal chemistry of the uranyl silicate minerals. *Am. Mineral.* **66**, 610-625.

SWIHART, G.H., GUPTA, P.K.S., SCHLEMPER, E.O., BACK, M.E. & GAINES, R.V. (1993): The crystal structure of moctezumite $[PbUO_2](TeO_3)_2$. *Am. Mineral.* **78**, 835-839.

TABACHENKO, V.V., BALASHOV, V.L., KOVBA, L.M. & SEREZHKIN, V.N. (1984a): Crystal structure of barium uranyl molybdate $Ba(UO_2)_3(MoO_4)_4\cdot 4H_2O$. *Koord. Khim.* **10**, 854-857 (in Russ.).

———, KOVBA, L.M. & SEREZHKIN, V.N. (1983): The crystal structure of molybdatouranylates of magnesium and zinc of composition $M(UO_2)_3(MoO_4)_4(H_2O)_8$ (M = Mg,Zn). *Koord. Khim.* **9**, 1568-1571 (in Russ.).

———, ——— & ——— (1984b): Crystal structures of $Mg(UO_2)_6(MoO_4)_7\cdot 18H_2O$ and $Sr(UO_2)_6(MoO_4)_7\cdot 15H_2O$. *Koord. Khim.* **10**, 558-562 (in Russ.).

———, ———, SEREZHKINA, L.B. & KOVBA, L.M. (1979): Crystal structure of manganese sulfatouranylate $MnUO_2(SO_4)_2\cdot 5H_2O$. *Koord. Khim.* **5**, 1563-1568 (in Russ.).

TALI, R., TABACHENKO, V.V. & KOVBA, L.M. (1993): Crystal structure of $Cu_4UO_2(MoO_4)_2(OH)_6$. *Zh. Neorg. Khim.* **38**, 1450-1452 (in Russ.).

TAYLOR, J.C. (1971): The structure of the α form of uranyl hydroxide. *Acta Crystallogr.* **B27**, 1088-1091.

——— & BANNISTER, M.J. (1972): A neutron diffraction study of the anisotropic thermal expansion of β-uranyl dihydroxide. *Acta Crystallogr.* **B28**, 2995-2999.

——— & MUELLER, M.H. (1965): A neutron diffraction study of uranyl nitrate hexahydrate. *Acta Crystallogr.* **19**, 536-543.

———, STUART, W.I. & MUMME, I.A. (1981): The crystal structure of curite. *J. Inorg. Nucl. Chem.* **43**, 2419-2423.

——— & WILSON, P.W. (1973): The structure of anhydrous uranyl chloride by powder neutron diffraction. *Acta Crystallogr.* **B29**, 1073-1076.

——— & ——— (1974): The structure of uranyl chloride monohydrate by neutron diffraction and the disorder of the water molecule. *Acta Crystallogr.* **B30**, 169-175.

TUTOV, A.G., PLAKHTII, V.P., USOV, O.A., BUBLYAEV, R.A. & CHERNENKOV, YU.P. (1991): Neutron diffraction refinement of the structure of a nonlinear optical crystal of dicaesiumuraniltetrachloride $Cs_2UO_2Cl_4$. *Kristallografiya* **36**, 1135-1138 (in Russ.).

VAN DER PUTTEN, N. & LOOPSTRA, B.O. (1974): Uranyl sulphate $2\frac{1}{2}H_2O\cdot UO_2SO_4\cdot 2\frac{1}{2}H_2O$. *Cryst. Struct. Commun.* **3**, 377-380.

VAN DUIVENBODEN, H.C. & IJDO, D.J.W. (1986): Redetermination of tricalcium uranate(VI). A Rietveld refinement of neutron powder diffraction data. *Acta Crystallogr.* **C42**, 523-525.

VAN EGMOND, A.B. (1976a): Investigations on cesium uranates. V. The crystal structures of Cs_2UO_4, $Cs_4U_5O_{17}$, $Cs_2U_7O_{22}$ and $Cs_2U_{15}O_{46}$. *J. Inorg. Nucl. Chem.* **38**, 1649-1651.

——— (1976b): Investigations on cesium uranates. VI. The crystal structures of $Cs_2U_2O_7$. *J. Inorg. Nucl. Chem.* **38**, 2105-2107.

VISWANATHAN, K. & HARNEIT, O. (1986): Refined crystal structure of β-uranophane $Ca(UO_2)_2(SiO_3OH)_2\cdot 5H_2O$. *Am. Mineral.* **71**, 1489-1493.

VOCHTEN, R., VAN HAVERBEKE, L., VAN SPRINGEL, K., BLATON, N. & PEETERS, O.M. (1995): The structure and physicochemical characteristics of synthetic zippeite. *Can. Mineral.* **33**, 1091-1101.

WELLER, M.T., DICKENS, P.G. & PENNY, D.J. (1988): The structure of δ-UO_3. *Polyhedron* **7**, 243-244.

WOLF, R. & HOPPE, R. (1985): Neues über Oxouranate: über α-Li_6UO_6. Mit einer Bemerkung über β-Li_6UO_6. *Z. Anorg. Allg. Chem.* **528**, 129-137.

_____ & _____ (1986): Neues über Oxouranate (VI): Na_4UO_5 und K_4UO_5. *Rev. Chim. Minérale* **23**, 828-848.

_____ & _____ (1987): Ein neues Oxouranat (VI): $K_2Li_4[UO_6]$. Mit einer Bemerkung über $Rb_2Li_4[UO_6]$ und $Cs_2Li_4[UO_6]$. *Z. Anorg. Allg. Chem.* **554**, 34-42.

WRONKIEWICZ, D.J., BATES, J.K., GERDING, T.J., VELECKIS, E. & TANI, B.S. (1992): Uranium release and secondary phase formation during unsaturated testing of UO_2 at 90°C. *J. Nucl. Mater.* **190**, 107-127.

YAMASHITA, T., FUJINO, T., MASAKI, N. & TAGAWA, H. (1981): The crystal structures of α- and β-$CdUO_4$. *J. Solid State Chem.* **37**, 133-139.

ZALKIN, A., RUBEN, H. & TEMPLETON, D.H. (1978): Structure of a new uranyl sulfate hydrate, α-$2UO_2SO_4 \cdot 7H_2O$. *Inorg. Chem.* **17**, 3701-3702.

_____, TEMPLETON, L.K. & TEMPLETON, D.H. (1989): Structure of rubidium uranyl(VI) trinitrate. *Acta Crystallogr.* **C45**, 810-811.

ZOLTAI, T. (1960): Classification of silicates and other minerals with tetrahedral structures. *Am. Mineral.* **45**, 960-973.

Received December 21, 1995, revised manuscript accepted April 16, 1996.